CRISPR/Cas9 technology abolishes the *BCR/ABL1* oncogene effect in chronic myeloid leukemia and restores normal hematopoiesis

Elena Vuelta[1,2,3], José Luis Ordoñez[1,4], Verónica Alonso-Pérez[1,4], Lucía Méndez[3], Patricia Hernández-Carabias[3], Raquel Saldaña[5], Julián Sevilla[6], Elena Sebastian[6], Sandra Muntión[1,2,6,8], Fermín Sánchez-Guijo[1,2,6,8], Jesús María Hernadez-Rivas[2,4,7], Ignacio García-Tuñón[1,4]* and Manuel Sánchez-Martín[2,3,4]*.

*These authors share the senior authorship.
Correspondence should be addressed to: ignacio.tunon@usal.es; adolsan@usal.es

[1]Unidad de Diagnóstico Molecular y Celular del Cáncer, Instituto Biología Molecular y Celular del Cáncer (USAL/CSIC), Salamanca, Spain.
[2]Departamento de Medicina, Universidad de Salamanca, Salamanca, Spain.
[3]Servicio de Transgénesis, NUCLEUS, Universidad de Salamanca, Salamanca, Spain.
[4]IBSAL, Instituto de Investigación Biomédica de Salamanca, Salamanca, Spain.
[5]Servicio de Hematología, Hospital de Especialidades de Jerez, Spain.
[6]Hospital Infantil Universitario Niño Jesús, Madrid, Spain.
[7]Servicio de Hematología, Hospital Universitario de Salamanca, Salamanca, Spain.
[8]RETIC TerCel y CIBERONC, ISCIII, Madrid, Spain.

Running head: CRISPR/Cas9 for gene therapy in CML.

Key Words: Chronic myeloid leukemia, BCR/ABL, CRISPR/Cas9, gene therapy, mouse model.

ABSTRACT

Chronic myeloid leukemia (CML) is a hematopoietic stem cell disease produced by a unique oncogenic event involving the constitutively active tyrosine kinase (TK) BCR-ABL1. TK activity explains most features of CML, such as tumor development and maintenance. TK-inhibitory (TKI) drugs have changed its prognosis and natural history. Unfortunately, since ABL1 gene remains unaffected by TKIs, most patients should be treated with lifelong oral medication, resistant mutations arise and adverse effects occur during treatment in almost 25% of patients To address this problem, we have designed a potentially definitive therapeutic alternative with CRISPR/Cas9 genome editing nucleases that target leukemic stem cells (LSCs). CRISPR-edited LSCs lose their tumorigenic capacity and restore their own multipotency. The strategy was evaluated for the first time in a CML mouse model and in orthotopic assays with primary LSCs from CML patients. In Both systems, CRISPR-edited LSCs repopulated and restored the normal hematopoiesis in immunodeficient NSG niches providing a significant therapeutic benefit. We show for the first time how CRISPR technology permanently interrupts and avoids the *BCR/ABL1* oncogene expression in human and mouse LSCs suggesting that human CML is an ideal candidate for CRISPR therapy, and providing proof-of-principle for genome editing in CML patients.

INTRODUCTION

Chronic myeloid leukemia (CML) was the first neoplastic disease to be associated with a chromosomal abnormality: a reciprocal translocation between chromosomes 9 and 22 (1,2). Since that discovery in 1962, a considerable number of fusion genes have been detected in malignant disorders that arise in the mesenchymal cell compartment. Most of these fusions are closely related to the pathogenesis of specific sub-types of leukemias, lymphomas or sarcomas (3).

One of the best characterized gene fusions is the BCR-ABL1 translocation, which is involved in the genesis of CML (4). CML is a human hematopoietic stem cell (HSC) disorder in which BCR-ABL1 oncoprotein drives the maintenance of the disease (5–8). This oncoprotein has a constitutively active tyrosine kinase (TK) that leads to the pathogenesis of CML (9,10). In contrast to other tumors such as carcinomas, the presence of BCR-ABL1 can explain most of the cellular features of the leukemia (enhanced cell growth, inhibition of apoptosis, altered cell adhesion, growth-factor independence, impaired genomic surveillance and differentiation), although in advanced-phases (accelerated phase and blast crisis) some of the mechanisms involved are BCR-independent (11).

TK activity leads to oligomerization of the coiled coil region (12) and deletion of the inhibitory SH3 domain of ABL (13). In turn, this results in autophosphorylation of the Y-177 tyrosine residue (14), recruitment of GRB2, activation of the RAS pathway (7,15–17), and phosphorylation of the JAK2 and STAT1/STAT5 proteins that transfer abnormal signals to the nucleus (18–21). This aberrant kinase signaling activates downstream targets that reprogram the cell to cause uncontrolled proliferation and a myeloid differentiation bias. The initial phase of the disease with no evident symptoms is known as the chronic phase (CP), and is normally characterized by the accumulation of myeloid cells in the bone marrow, peripheral blood, and, less frequently, other sites in the body without a blockade of myeloid progenitor cell differentiation. Without an effective treatment, the CP evolves to an aggressive phase called the blast crisis (BC), which is characterized by the blockage of hematopoietic differentiation and accumulation of immature blast cells, resembling acute leukemia. At this stage, the natural course of the disease takes on an aggressive phenotype and is almost always fatal, except for the few patients in whom an allogeneic hematopoietic stem cell transplant succeeds in eradicating the disease. About 70% of cases develop acute myeloblastic leukemia (AML), and approximately 20–30% of patients develop lymphoblastic leukemia (22). BC triggers a bone marrow failure, and massive infiltration with immature blasts leads to patient mortality from infection, thrombosis or anemia. Before successful TKI treatment, the median survival of CML patients after diagnosis was approximately 3 years (23,24). Until the 1980s, patients were treated with arsenic, radiotherapy, busulfan and hydroxyurea, but had a poor outcome. Between the 1980s and 2000, most patients received IFN-α-based therapy if they presented with CP, or combinations of IFN-α and chemotherapy if they presented with

BC. As a result, the median survival doubled to 6 years. Finally, with the development of tyrosine kinase inhibitors (TKIs) the therapeutic options for treating CML have changed markedly.

In CP-CML patients, the estimated 8-year survival has improved from a historic rate of less than 20% to the current rate of 87%, with sustained survival and a low risk of progression (23,25), and life expectancy is almost identical to that of the healthy population of the same age(26). The results provided strong evidence for a critical role for BCR-ABL kinase activity in CML pathogenesis, and demonstrated the potential for the development of anticancer drugs based on the specific oncogenes that drive human malignancies (27). However, despite successful outcomes in CP-CML patients, TKI resistance is observed in approximately 25% of patients, mainly due to mutations in the BCR-ABL1 fusion gene. Other patients experience relapse after initial success (28). Except for a subgroup of patients who achieve a deep and sustained molecular response, TKI therapies need to be continued indefinitely because they do not completely eliminate the leukemic stem cells that remain "oncogenic-quiescent" during the treatment (29). Therefore, it is still necessary to seek new therapeutic alternatives, especially for TKI-resistant patients.

The recently developed clustered regularly interspaced short palindromic repeats (CRISPR)/Cas9 system, which is widely used for genome editing in all organisms (30–32), could be a definitive therapeutic option for these patients. CRISPR therapies based on specific oncogenic silencing within hematopoietic leukemic stem cells (LSCs) may be the best example of these. In this pathological cell context, the highly efficient interruption of the oncogenic open reading frame might be an effective therapeutic option, especially for tumors that are directed by a single oncogenic event, such as BCR-ABL1traslocation (33,34). Furthermore, the CRISPR/Cas9 system works at the DNA level and has the advantage of providing complete and permanent oncogene knockout, while TKIs only ensure that BCR-ABL1 is inactivated during treatment. CRISPR/Cas9 cuts DNA in a sequence-specific manner with the possibility of interrupting the ABL1 TK sequence, thereby making it possible to turn off the oncogenic activity in a way that was not previously feasible in humans (35). However, it remains unresolved whether leukemic stem cells, once edited by the CRISPR system, can restore normal hematopoiesis and be assessed in clinical trials.

The present work demonstrates that CRISPR-Cas9 technology efficiently targets mouse and human LSCs, and that the edited cells engraft into NSG bone marrow. More importantly, the tumorigenic capacity of edited cells is abolished, but they have the ability to restore normal hematopoiesis. CRISPR-edited human and mouse LSCs repopulated and restored normal hematopoiesis in immunodeficient NSG niches. The treatment has been evaluated in mouse models and in patient's primary cells and makes CML an ideal candidate for CRISPR therapy in cases for which TKIs are not effective. We show that CRISPR technology can be used to abrogate the *BCR/ABL1* oncogene in LSCs from CML cell lines, CML transgenic mice and human CML patients, restoring

normal hematopoiesis and bestowing a clinical benefit. Our study provides proof-of-principle for genome editing in CML patients.

RESULTS

1. The CRISPR/Cas9 deletion system efficiently disrupts the BCR/ABL oncogene, preventing its expression

The murine CML cell line Boff-p210 was electroporated with Cas9 RNP joined to two specific sgRNAs targeting the *ABL* TK domain at exon 6 (here named Boff-*ABL*-TK) or without sgRNAs as a control (Boff-Cas9). A 473-bp band corresponding to BCR/ABL genomic exon 6 was amplified by PCR in Boff-*ABL*-TK and Boff-Cas9 cells. As expected, an extra band of 372 bp was detected only in Boff-*ABL*-TK cells, suggesting the presence of a deletion generated by the action of both RNA guides (Figure 1A). Sanger sequencing revealed a mixture of sequences between the expected cleavage point of both guides (Figure 1B) and confirmed the specific deletion at expected Cas9 cut sites. To analyze the effect of this deletion, we made a single-cell seeding (SC) and isolated a single-cell-derived clone carrying the specific CRISPR deletion affecting the ABL1 TK domain (named SC-*ABL*-TK). PCR amplification of *ABL* exon 6 showed a single band of 368 bp in SC-*ABL*-TK cells, in contrast with a 469-bp unedited band observed in SC-Cas9 cells, suggesting the presence of a specific CRISPR deletion in *ABL* loci (Figure 1A). The specific 101-bp deletion was confirmed by Sanger sequencing in Boff-*ABL*-TK and SC-*ABL*-TK (Figure 1B). To determine the relevance of the 101-bp DNA deletion at the mRNA and protein levels, ABL expression was quantified by RT-PCR. As expected, SC-*ABL*-TK cells showed a shorter human *ABL* mRNA than full-length sequences (Figure 1C). Sanger sequencing of the RT-PCR products showed a mRNA carrying a 101-bp deletion in the edited SC-*ABL*-TK cells. *In silico* analysis of the truncated ABL mRNA showed a 101-bp deletion that gives rise to a frameshift mutation due to a premature STOP codon at the contiguous *ABL* exon 7 (Figure 1C). To determine whether the frameshift mutation triggers mRNA decay, a qPCR was performed using oligos located downstream from the deletion region (the exon 7-8 junction; Table S1). SC-ABL-TK cells showed a statistically significant lower level of expression (2.6%, $p<0.001$) compared with SC-Cas9 control cells (Figure 1D). These data were confirmed by western blot using an ABL antibody to detect human ABL protein expression in cells. While Boff-Cas9 and SC-Cas9 cells normally expressed a 250-kDa BCR/ABL protein, SC-*ABL*-TK edited cells showed no expression of BCR/ABL protein similar to BCR/ABL-negative BaF/3 cells (Figure 1E).

To establish whether these results are also reproducible in human cells, the human CML-derived cell line K562 was electroporated with Cas9 RNP joined to two TK sgRNAs targeting *BCR/ABL* exon 6. A 473-bp band corresponding to BCR/ABL genomic exon 6 was amplified by PCR in K562-Cas9 cells (control) and K562-ABL-TK cells. As expected, an extra band of 372 bp was amplified in the edited cells, which was consistent with CRISPR-induced deletion (Figure 2A). Sanger sequencing showed a mixture of sequences between the expected cleavage points of both guides (Figure 2A) and confirmed the specific deletion at the expected Cas9 cut sites.

BCR/ABL oncogene expression was determined by qPCR (Figure 2B), which revealed significantly ($p<0.001$) lower BCR/ABL mRNA levels in K562 *ABL*-TK cells than in the two control cell lines (parental and Cas9 cells). Western blot analysis of ABL and BCR-ABL proteins in K562 *ABL*-TK cells confirmed the lower level of expression of both proteins compared with the K562-Cas9 control cells (Figure 2C). The ABL immunofluorescence assay detected a huge decrease in BCR/ABL-positive cells in the K562 *ABL*-TK cell pool (Figure 2C).

2. The CRISPR/Cas9 deletion system abolishes the BCR/ABL oncogenic effect in murine and human CML cell lines

To determine the biological significance of disrupting the coding sequence of *BCR/ABL* with the CRISPR system at ABL1 TK domain, we analyzed the apoptosis levels and DNA content of edited and control cells. Unlike BaF3 (Boff parental cells), Boff-p210 cells are IL-3-independent of growth and survival due to the oncogene signaling. Thus, we studied the effect of abrogating *BCR/ABL* by CRISPR in Boff-p210 cells in the absence of IL-3 (Figure 3). 48 hours after electroporation and IL-3 withdrawal, we observed a basal level of mortality of 15.1% (annexin V-positive cells) similar to the observed in IL3 presence (13.3%) in SC-Cas9, while this level reached 99.1% on average in the SC-ABL-TK cells (Figure 3A). Accordingly, we also observed a 94.5% of SubG0 DNA content cells in SC-*ABL*-TK with respect to unedited SC-Cas9 cells (2.1%) (Figure 3B).

For the human cell line, we analyzed the level of apoptosis and the DNA content in human K562-Cas9-TK cells (Figure 4). We also detected a significant ($p<0.001$) increase in the percentage of annexin V-positive cells (63.2%) in K562 *ABL*-TK-edited cells, while K562 (parental) and K562-Cas9 cells showed lower levels (8.4% and 14.5%, respectively) (Figure 4A, 4B). DNA content analysis (propidium iodide) of K562-Cas9-TKs cells showed 24.6% of SubG0 cells, while K562 (parental) and K562-Cas9 control cells showed 1.76% and 4.87% of SubG0 cells, respectively (Figure 4C).

3. CRISPR/Cas9 deletion system abolishes BCR/ABL oncogene expression in primary murine CML leukemic stem cells, which restore their own multipotent capacity and impair the myeloid bias

To address whether a primary murine CML stem cell, edited with the CRISPR/Cas9 system to abolish ABL1 expression, re-acquires its multipotent capacity, we used a CML transgenic mouse expressing BCR/ABL1 human oncogene (36). Lin^- primary leukemic stem cells (mLSCs) were isolated from CML transgenic mice with symptomatic chronic disease (>60% $Gr1^+$ cells in peripheral blood). BCR/ABL transgene sequence was disrupted by electroporation of Cas9 RNP joined to *ABL*-TK sgRNAs targeting the TK domain at exon 6. PCR amplification of *ABL* exon 6 at mLSCs-*ABL*-TK cells showed specific 469-bp and 368-bp bands, while a single band (469 bp) was observed in mLSCs control cells (Figure 5A). Sanger sequencing displayed a mixture of sequences at the CRISPR-Cas9 target region in mLSCs-*ABL*-

TK cells (Figure 5A). PCR-cloning and sequencing demonstrated the specific 101-bp deletion between Cas9 cleavage points.

Total mRNA from electroporated mLSCs-*ABL*-TK cells was isolated and the expression level of BCR/ABL quantified by qPCR (Figure 5B). While mLSCs-Cas9 control cells showed high BCR/ABL mRNA levels, we found significantly ($p<0.001$) lower levels of expression in mLSCs-Cas9 cells. Accordingly, a markedly lower levels of ABL protein were detected by immunofluorescence in mLSCs-*ABL*-TK cells (Figure 5C).

To test the multipotency of these mLSCs-*ABL*-TK cells we transplanted them and their counterpart mLSCs-Cas9 cells into two irradiated immunodeficient NSG mice (NSG-Cas9 and NSG-*ABL*-TK; Figure 6A). Several hematopoietic cell lineages from the peripheral blood of transplanted NSGs were analyzed 120 days post-transplant (Figure 6B). Significantly, we detected and isolated specific hematopoietic cells populations such as myeloid cells ($Gr1^+$), B lymphocytes ($B220^+$) and T lymphocytes ($CD4^+$ or CD8), arising from both NSG-ABL-TK and NSG-Cas9 mice. In contrast, FACs analysis only detected normal white cell percentages in peripheral blood from NSG-*ABL*-TK, while the NSG-Cas9 counterpart exhibited a $Gr1^+$ bias to the detriment of the lymphoid linage (Figure 6B). As expected, PCR amplification of ABL exon 6 in all sorted populations from NSG-*ABL*-TK showed the presence only of the CRISPR/Cas9 ABL1 (Figure 6C). Importantly, compared with NSG-Cas9, a smaller $Gr1^+$ population was detected in NSG-ABL-TK, at least during the first 60 days post-transplant. The *BCR/ABL* qPCR assay in sorted $CD45^+$ cells from NSG-ABL-TKs at 120 days post-transplant showed a lower level of expression (69.1 ± 1.9%) than its NSG-Cas9 counterpart (Figure 6D).

4. mLSCs modified by CRISPR at the ABL1 locus impairs the myeloid bias, restoring normal hematopoiesis

To determine whether LSC-*ABL*-TK could be potentially useful as a CML therapy, 12 independent NSG bone marrow transplantation assays of mLSCs CRISPR-edited and non-edited were performed (Figure 7). Four groups of mice were studied: 1) six NSG mice with CRISPR-edited mLSCs from CML donors (NSG-*ABL*-TK), 2) six NSG mice with non-edited mLSCs from CML donors (NSG-Cas9), 3) five CML transgenic mice, used as parental disease controls (CML-Tg), and 4) five wildtype mice, used as normal controls (WT) (Figure 7A). All mLSCs were isolated from bone marrows of at least one-year-old CML transgenic mice with clinical disease (>60% $Gr1^+$ cells in peripheral blood) (Table S2). The BCR/ABL transgene sequence was CRISPR-disrupted in Lin^- mLSCs, as described above. CRISPR/Cas9-specific deletion at the *ABL1* TK domain was confirmed by PCR and Sanger sequencing. Peripheral blood cell analysis by FACs was performed 2 months after transplant to study the hematological cell populations. The end-point was determined at 4 months.

We observed that four of the six NSG-Cas9 mice suffered splenomegaly, as was observed in CML transgenic mice. However, the spleens of all the NSG-*ABL*-TK were of normal size compared with those of WT mice (Figure 7B).

The proportion of Gr1+ cells increased in all NSG-Cas9 mice, reaching 59.2 ± 9.9% in peripheral blood by the end-point. In contrast, a significantly lower percentage of $Gr1^+$ cells was detected in NSG-ABL-TKs (29.2 ± 6.6; $p<0.001$), similar to what was observed in WT mice (17.9 ± 3.4) (Figure 7C-7D). There was a significantly higher percentage of $Mac1^+$ cells (55.2 ± 8.2) in NSG-Cas9 than the normal levels seen in NSG-ABL-TK (31.7 ± 5.7; $p<0.05$) and WT mice (19.6 ± 1.5; $p<0.05$). As expected, there were low levels of aberrant lymphoid cell populations in NSG-Cas9 and CML mice (Figure 7C-7D).

To study in greater detail the how the time to evolution of the $Gr1^+$ cell population is related to disease stages while accounting for interindividual differences among donors, three independent transplantation assays were performed with three independent mLSC donor mice (Table S2; Figure 7E). The different clinical disease stages were defined as "initial phase" (donor #1, $Gr1^+$ ≤40%), "chronic phase" (donor #2, $Gr1^+$ ≥40% and ≤60%), and "advanced phase" (donor #3, $Gr1^+$ ≥ 60%). LSCs from each CML mouse were divided in two samples and electroporated with or without all CRISPR reagents (NSG-*ABL*-TK and NSG-Cas9). Both samples were transplanted into NSG receptors and maintained for 6 months (Figure 7E). At the time of transplantation, the CML donor mice selected showed 35.4% (donor#1), 52.3% (donor#2) and 63.9% (donor#3) of $Gr1^+$ cells. 4 months after transplantation, all NSG-*ABL*-TKs mice had normal levels of $Gr1^+$ cells (donor#1, 23%; donor#2, 8%; donor#3, 35%) and were similar 6 months after transplantation. In contrast, all NSG-Cas9 mice showed increasing $Gr1^+$ populations at 2 months and reached pathological levels by the end-point (donor#1, 52%; donor#2, 62%; donor#3, 72%) (Figure 7E).

5. The CRISPR/Cas9 deletion system efficiently disrupts the BCR/ABL oncogene in $CD34^+$ LSCs from CML patients, impairing the myeloid bias and restoring its normal multipotency

To corroborate the applicability of CRISPR technology as a potential therapeutic tool in human CML, LSCs $CD34^+$ were isolated from 17 CML patients at diagnosis in the chronic phase. Similar to the assays described above, we electroporated $CD34^+$ hLSCs with Cas9 RNP, with or without two specific sgRNAs targeting the *BCR/ABL* exon 6 (hLSCs-*ABL*-TK and hLSCs-Cas9). A 473-bp band, corresponding to BCR/ABL genomic exon 6, and an extra band of 372 bp were also detected by PCR in hLSC-*ABL*-TKs. As expected, a single 473-bp band was amplified in hLSCs-Cas9 and control $CD34^+$ cells (Figure 8A). Sanger sequencing confirmed the specific deletion between the expected Cas9 cut sites (Figure 8A). Quantitative PCR of mRNA from hLSCs-*ABL*-TKs showed a significantly lower level of expression of *BCR/ABL* mRNA ($p<0.001$) than in controls (Figure 8B). These results were confirmed by western blot (Figure 8C).

To explore the ability of the CRISPR/Cas9 system to abolish the tumorigenic capacity of hLSCs, we studied proliferation and survival of hLSC-*ABL*-TK cells *in vitro* (Figure 8D). hLSC-*ABL*-TK had a lower proliferation rate than did hLSC-Cas9 cells. Accordingly, hLSC-*ABL*-TK also showed a higher percentage of cell death than did hLSC-Cas9 cells (Figure 8D).

Similar to what was found in previous animal assays, 17 CML $CD34^+$ cell samples from patients at diagnosis in the chronic phase were included (Table S3) and divided into three groups: seven that were electroporated with Cas9 and *ABL1* sgRNAs (hLSC-*ABL*-TKs), seven that were electroporated solely with Cas9 (hLSCs-Cas9), and three un-electroporated CML $CD34^+$ cells as controls. Three healthy donors were used as controls (NSG-healthy-$hCD34^+$). A total of 20 NSG mice of the same age were used as receptors of these cells (Figure 9A). A representative FACS analysis of bone marrow 4 months after transplantation is shown in Figure 9B. In all cases, the percentages of myeloid cells (hCD14 and hCD117) and lymphoid B cells (hCD19) in NSG-hLSC-*ABL*-TK were normal. mRNA from $hCD45^+$-sorted bone marrow cells was isolated from NSG-hLSC-Cas9 and NSG-ABL-TKs mice to analyze *BCR/ABL* expression by qPCR (Figure 9C). NSG-hLSC-*ABL*-TK presented significantly lower levels of expression of BCR/ABL and ABL (30.3 ± 12.5% and 33.2 ± 17.7%, respectively; $p<0.01$) than did NSG-hLSC-Cas9 mice (Figure 9C).

FACS analysis of human hematological populations from NSG bone marrow samples was carried out 6 months after transplantation (Figure 9D), which revealed normal levels of $hCD14^+$ (5.4 ± 2.6%), $hCD117^+$ (15.5 ± 8.7%) and $hCD19^+$ (84.9 ± 3.9%) in all NSG-hLSC-*ABL*-TK. In contrast, higher levels of $CD14^+$ (65.1 ± 12.7%) and $CD117^+$ (86.5 ± 5.1%), and reduced levels of $hCD19^+$ (15.1 ± 3.7%) were detected in all NSG-hLSC-Cas9 bone marrow samples ($p<0.001$). (Figure 9D).

A linear regression analysis of $hCD117^+$ and $hCD19^+$ cell populations in the NSG mice engraftments showed an inverse correlation ($r^2 = 0.9212$) among NSG-hLSC-*ABL*-TK and NSG-healthy-hCD34+ with respect to NSG-hLSC-Cas9 and NSG-hLSC $CD34^+$ donors (Figure 9E).

DISCUSSION

As our understanding of the molecular pathogenesis of CML has developed, its prognosis has improved, from being that of a fatal disease, to one of a chronic disorder that can be treated with lifelong oral medication that could be even discontinued in a small subset of patients (37). This change has been possible due to the development of targeted drugs, such as TKIs, that inhibit the oncoprotein. Unfortunately, these drugs do not tackle the fundamental cause of the disease, and the oncogenic event remains unaffected or uncorrected. Thus, lifelong oral medication is necessary for most CML

patients, and a significant percentage of patients eventually become resistant to TKI treatment (38).

Currently, an oncogenic event can be easily abolished by using CRISPR/Cas9 nucleases, which offers a new and definitive opportunity for TKI-resistant CML patients (33,34). Our study demonstrates the effectiveness of CRISPR-Cas9 for knocking out BCR/ABL1, a key oncogene in the CML process. In this study, CRISPR/Cas9 has been used *in vitro* to interrupt the ABL1 sequence and to abolish its expression. To ensure a null oncogenic effect, we designed two sgRNAs to induce a specific short deletion at the TK domain of ABL1, which is responsible for BCR/ABL1 activity. Furthermore, this deletion allows the tracking of edited LSCs and their daughter cells. We have shown that edited cells, of the CML cell line or the primary mouse/human LSCs, lose their survival and proliferation properties. We found a complete absence of BCR/ABL expression in single-edited-cell clones and a significant reduction in edited CML cell lines and primary LSCs from mice and human patients. The absence or reduced level of BCR/ABL1 expression was corroborated at the protein level and triggered cellular apoptosis, particularly in the edited CML cell lines, and stopped proliferation, especially in primary edited LSC samples. Together, these results indicate that CRISPR/Cas9 could be used to generate ABL1 null alleles and to abolish or reduce BCR/ABL1 transcripts in all types of cell sample, thereby preventing any oncogenic effect on survival and proliferation.

However, critical questions about using CRISPR as a new potential tool for CML treatment remain, such as whether CRISPR-edited LSCs can engraft and dominate bone marrow hematopoiesis or, if the edited LSC recovers its multipotential commitment and thereby avoids the myeloid bias. To address these questions, we performed several mouse-mouse and human-mouse BMT assays using immunodeficient NSG as the best recipient for studying the multipotency of human and mouse hematopoietic stem cells *in vivo* (39). A humanized transgenic mouse for mimicking CML was used as an LSC donor to test the engraftment capacity and multipotency of CRISPR-edited mLSCs. We noted the presence, 120 days after BMT, of $CD45^+$ cells arising from the edited mLSCs with the CRISPR-induced *ABL1* deletion. In contrast to NSG-Cas9 controls, we detected normal percentages of myeloid and lymphoid cells in NSG-*ABL*-TK due to the multilineage capacity of the CRISPR-edited mLSC. Importantly, myeloid bias was not detected in NSG-*ABL*-TK, at least 120 days after BMT, which suggests that CRISPR electroporation significantly reduces the tumor burden. No clinical symptoms or splenomegaly were detected in all NSG-*ABL*-TKs, unlike what we observed in NSG-Cas9 and CML-Tg mice. To study the evolution of BMTs with respect to disease stage, which is related to tumor burden, we measured the $Gr1^+$ percentage at the beginning, and 60 and 180 days post-BMT. We detected higher percentages of $Gr1^+$ tumoral cells in all NSG-Cas9 controls. In contrast, 180 days post-BMT, all NSG-*ABL*-TK mice showed lower levels of $Gr1^+$ cells than those detected at the start. Therefore, we concluded that the CRISPR deletion system restored normal hematopoiesis and produced a therapeutic benefit in

the CML mouse model. To determine whether that result was reproducible, similar BMT assays were performed with CML human samples collected from untreated chronic-phase CML patients. Successful engraftment was defined as the presence of at least 0.1% human $CD45^+$ cells in bone marrow, measured by flow cytometry (40). All NSG mice included in this study presented engraftments between 0.7 % and 9.4 %, whereby migration and self-renewal capacity of the transplanted cells (edited and non-edited) were not affected. As expected, we detected normal hematopoiesis in all NSG-hLSC-*ABL*-TK mice, similar to what was found in NSG-healthy $CD34^+$ cases, and as other authors have noted in NSG with human HSC engraftments from healthy controls (41). Normal hematopoiesis is defined by a high proportion of B cells, very low levels of T cells, and the absence of myeloid bias. In contrast, all NSG-hLSC-Cas9 developed a myeloproliferative disorder in a similar way as occurs in NSG-hLSC $CD34^+$, with a high proportion of $CD14^+$ and $CD117^+$ cells. CD117 and CD19 expression were negatively correlated when all the engraftments at 6 months were analyzed, implying that CD117+ expression is associated with the myeloid phenotype and/or the progression of CML.

Our results show that CRISPR/Cas9 technology could provide the basis for a very useful alternative drug for treating human CML and is the first step towards providing proof-of-principle for genome editing of the main genetic event in CML patients.

Material and Methods

BCR/ABL1 in silico analysis and CRISPR/Cas9 system design and reagents

In most CML patients, the point of fusion in BCR is located on the major region (M-bcr) downstream of exons 13 or 14, whereas the break-point of the ABL gene is generally located upstream of the second exon (a2) (42,43). This translocation produces a 210 kDa chimeric protein containing BCR as an N-terminal fusion partner joined to SH-domains, proline-rich (PxxP), nuclear localization signal (NLS), DNA-binding, nuclear export signal (NES) and actin-binding domains of ABL (44,45) (Figure S1).

In order to destroy the BCR-ABL TK domain and thereby prevent Tk activity, we designed two sgRNAs (*ABL* TK1-sgRNA and *ABL* TK2-sgRNA) (Table S1). To easily detect and track the edited leukemic cells, both sgRNAs were designed to generate a small deletion (101 bp) targeting the *ABL* exon 6, destroying the ABL TK domain, and triggering a downstream frameshift mutation (Figure S1). TK-sgRNA sequences, were designed with the Spanish National Biotechnology Centre (CNB)-CSIC web tool BreakingCas (http://bioinfogp.cnb.csic.es/tools/breakingcas/).

Mouse model, cell lines, cell samples, isolation, electroporation and culture conditions

The transgenic mouse model TgP210, developed by Honda et al. (36), expresses the human cDNA of *BCR/ABL*p210, which is controlled by the hematopoietic stem cell *Tec* promoter, mimicking human CML disease.

Boff-p210 is a murine interleukin 3 (IL3)-independent cell line derived from the hematopoietic cell line Baf/3(46) that expresses the *BCR/ABL* cDNA transgene (47–49). Boff-p210 was maintained in Dulbecco's Modified Eagle's Medium (DMEM) (Gibco, Thermo Fisher Scientific, CA, USA) supplemented with 10% FBS and 1% penicillin/streptomycin (Thermo Fisher Scientific, CA, USA). IL-3-dependent Baf/3 cells, used as a parental cell line, were grown in the same medium supplemented with 20% WEHI-3-conditioned medium as a source of IL-3.

The human CML-derived cell line K562 was purchased from the DMSZ collection (Leibniz-Institut DSMZ-Deutsche Sammlung von Mikroorganismen und Zellkulturen GmbH, Germany). K562 cells were cultured in RPMI 1640 medium (Gibco, Thermo Fisher Scientific, CA, USA) supplemented with 10% FBS, and 1% penicillin/streptomycin (Thermo Fisher Scientific, CA, USA). All cell lines were incubated at 37°C in a 5% CO_2 atmosphere. The presence of mycoplasma was tested for frequently in all cell lines with a MycoAlert kit (Lonza, Switzerland), exclusively using mycoplasma-free cells in all the experiments carried out.

Mouse hematopoietic cells were isolated from mouse bone marrow samples by flushing their femurs with a syringe containing 2 mL PBS–10% FBS. After red blood lysis treatment, AutoMACs sorter with a Direct Lineage Cell Depletion Kit mouse (MiltenyiBiotech, Germany) was used to separate Lin^- stem cells, which were then maintained in culture for 24 h in IMDM (Gibco, Thermo Fisher Scientific, CA, USA) supplemented with 2% fetal bovine serum, interleukin-3 (mIL-3; 10 µg/mL), interleukin-6 (mIL-6; 10 µg/mL), and thrombopoietin (mTPO; 10 µg/mL) and stem cell growth factor (mSCF; 10 µg/mL) (Preprotech EC Ltd., UK). Mice were housed in a temperature-controlled specific pathogen-free (spf) facility using individually ventilated cages, standard diet and a 12 h light/dark cycle, according to EU laws, at the Servicio de Experimentación Animal at the University of Salamanca.

Human $CD34^+$ cells were isolated from patient bone marrow samples by erythrocyte lysis buffer treatment, followed by separation with AutoMACs sorter and CD34 Microbead Kit human (MiltenyiBiotech, Germany) and grown in IMDM (Gibco, Thermo Fisher Scientific, CA, USA) supplemented with 2% FBS (Gibco, Thermo Fisher Scientific, CA, USA), interleukin-3 (hIL-3; 10 µg/mL), interleukin-6 (hIL-6; 10 µg/mL), and thrombopoietin (hTPO) (10 µg/mL), stem cell growth factor (hSCF; 10 µg/mL) and Fms-related tyrosine kinase 3 ligand (hFlt3-L; 10 µg/mL) (Preprotech EC Ltd, UK). $CD34^+$ cells were maintained in culture for 24 h before electroporation.

CRISPR/Cas9 ribonucleocomplex assembly and electroporation

The guide RNAs against ABL TK domains were composed by annealing equimolar concentrations of crRNA (specific target sequence; Integrated DNA Technology, Belgium) and of tracrRNA to a final duplex concentration of 44 µM by heating at 95ºC for 5 min and ramp down temperature to 25ºC. 22 pmol of duplex was incubated with 18 pmol of Cas9 enzyme (Integrated DNA Technology, Belgium) to final volume of 1 µL for electroporation. We added 2 µL of 10.8 µM of Electroporation Enhancer (Integrated DNA Technology, Belgium), and 9 µL of cell suspension of 3 x 10^7 cells/mL.

Cells were electroporated using Neon Transfection System 10 µL Kit (Invitrogen, Thermo Fisher Scientific, CA, USA) following the manufacturer's instructions. The electroporation parameters for each cell type are described in the following table:

Cells	**Pulse Voltage (v)**	**Pulse Width (ms)**	**Pulse Number**
Boff-p210	1700	2	1
K562	1450	10	3
$mLin^-$	1700	2	1
$hCD34^+$	1600	10	3

DNA and RNA insolation, amplification and genotyping

Genomic DNA from cells was extracted using the QIAamp DNA Micro Kit (Qiagen) following the manufacturer's protocol. To amplify the different target regions of human ABL-1, PCR was performed with the oligos described in Table 1.

PCR products were purified using a High Pure PCR Product Purification Kit (Roche) and sequenced by the Sanger method using forward and reverse PCR primers.

RT-PCR and quantitative PCR

To test BCR/ABL mRNA expression, 150 ng of total mRNA from cells were extracted by RNeasy mini kit (Quiagen, Germany) and *in vitro*-retrotranscribed using a SuperScript III First-Strand Synthesis Super Mix kit (Thermo Fisher Scientific, CA, USA). cDNA was used as a template to PCR-amplify the specific edited sequence of *BCR/ABL* exon 6 (Table S1). PCR product was purified and Sanger-sequenced.

BCR/ABL mRNA expression was quantified by qPCR (Applied Biosystems, CA, USA) using oligos targeting *BCR/ABL* Phusion point BCR/ABL qPCR F and BCR/ABL qPCR R. GAPDH mRNA expression was used as a control (oligos Gapdh qPCR F and R, Table S1).

Western blot and immunofluorescence

BCR-ABL protein expression was assessed by SDS-PAGE and western blotting using a mouse anti-ABL antibody (1:1,000, Santa Cruz Biotechnology, CA, USA). Horseradish peroxidase-conjugated α-mouse antibody (1:10,000; NA931V, GE Healthcare, IL, USA) was used as a secondary antibody. Antibodies were detected using ECL™ Western Blotting Detection Reagents (RPN2209, GE Healthcare, IL, USA). As a control, β-actin expression was measured using mouse anti-β-actin (1:20,000; Sigma Aldrich, USA).

For immunofluorescence analysis, cells were fixed and permeabilized onto poly-L lysine-coated slides as previously described (50). After blockade, slides were incubated with anti-ABL (Santa Cruz Biotechnology, CA, USA) antibodies at 1:1,000 dilution for 2 h. Cy™5 Goat Anti-Mouse (Jackson Immunoresearch, PA, USA) were used as secondary antibodies (1:1,000; 1 h). Nuclei were stained with DAPI (4′,6′-diamidine-2-fenilindol), diluted in PBS and incubated for 3 min with agitation at room temperature. Cells were washed twice in PBS and slides were mounted with Vectashield reagent (Vector Laboratories, CA, USA). Images were acquired using a Leica TCS SP5DMI-6000B confocal microscope (Leica Biosystems, Germany).

Apoptosis and cell-cycle analysis

Apoptosis was measured by flow cytometry with an annexin V-Dy634 apoptosis detection kit (ANXVVKDY, Immunostep, Spain) following the manufacturer's instructions. Briefly, 5×10^5 cells were collected and washed twice in PBS, and labeled

with annexin V-DY-634 and non-vital dye propidium iodide (PI), to enable the discrimination of living cells (annexin-negative, PI-negative), early apoptotic cells (annexin-positive, PI-negative) and late apoptotic or necrotic cells (annexin-positive, PI-positive). In parallel, cell distribution in the cell cycle phase was also analyzed by measuring DNA content (PI labeling after cell permeabilization). Data were analyzed using FlowJo software (vX.0.7. TreeStar, OR, USA).

Flow cytometry analysis and cell sorting for Cas9-mediated editing and for isolating single edited cell-derived clones

Boff-p210 cells were selected by fluorescence-activated cell sorting (FACS) using FACS Aria (BD Biosciences, CA, USA) 48 h after electroporation with a CRISPR/Cas9 system composed of two *ABL*-TKs crRNA and fluorescent ATTO-labeled tracRNA (Integrated DNA Technology, Belgium). Single cells were seeded in a 96-well plate establishing the SC-*ABL*-TK and SC-Cas9 clones, the latter being used as a control.

Hematopoietic stem cell transplantation

After 24 h in cytokine enriched culture, 1.8 x 10^6 Lin^- cells from $Tgp210^+$ C57BL/6 mice, or human $CD34^+$ cells from the CML bone marrow sample, were divided to undergo only Cas9 (used as control) or full CRISPR system (Cas9 and *ABL*-TK sgRNAs) electroporation.

As a control of CML disease and normal hematopoiesis, $Tgp210^+$ and C57BL/6J wild type mouse were used. In human-mouse bone marrow transplantation, we used 9 x 10^5 $hCD34^+$ cells without electroporation from CML patients and healthy donors as controls.

Electroporated and non-electroporated HSC cells were injected intravenously through the lateral tail vein in sublethally irradiated NSG (NOD scid gamma, Charles River) 4-5-week-old mice (2 Gy, 4 h before injection). Mice were irradiated at the Radioactive Isotopes and Radioprotection service of NUCLEUS, University of Salamanca. Mice were sacrificed by anesthetic overdose 4 or 6 months after cell injection.

Flow cytometry analysis

Four months after mouse-mouse bone marrow transplantation, recipient mice were euthanized and flow cytometric analysis of peripheral blood was carried out. Red blood cells were lysed with erythrocyte lysis buffer, and the remaining cells were washed twice in PBS. Samples were stained with fluorophore-conjugated antibodies against anti-mCD45 (PerCP-Cy5), anti-mB220 (PE), anti-mIgM (APC), anti-mCD4 (FITC), anti-mCD8 (APC) (all from Biolegend, CA, USA), and against anti-Gr1 (APC-Cy7), anti-Mac (FITC), anti-sca1 (PE) and anti-ckit (PE-Cy7 (all from BD Biosciences, CA, USA).

In human-mouse bone marrow transplantation, recipient mice were euthanized 24 weeks after cell injection. Bone marrow was extracted by flushing tibia and femurs, and red cells were lysed. The remaining cells were stained with fluorophore-conjugated antibodies against anti-hCD45 (FITC), anti-hCD34 (APC), anti-hCD14 (APC-H7), anti-hCD15 (FITC) (all from BD Biosciences, CA, USA), anti-mCD45 (PerCP-Cy5, Biolegend CA, USA), and anti-hCD19 (PE-Cy7, Immunostep, Spain). Samples were obtained on a FACSAria flow cytometer (BD Biosciences CA, USA) and data were analyzed using FlowJo software (TreeStar, OR, USA).

Statistical analysis

Statistical analyses were performed using GraphPad Prism 6 Software (GraphPad Software). Group differences between levels of annexin V labeling and BCR/ABL expression were tested with one- and two-way ANOVA, respectively, and Tukey's multiple comparisons test. Differences in percentages of hematological populations were estimated by two-way ANOVA. Statistical significance was concluded for values of $p < 0.05$ (**) and $p < 0.001$ (***).

Ethics statement

The study with human samples and human data followed the Spanish Biomedical Research Law 14/2007, RD 1716/2011, RD 1720/2007 and European Regulation 2016/679 (General Data Protection Regulation). The study was approved by the Ethics Committee for research in human drugs (CEIC) of IBSAL, Salamanca, Spain (reference PI5505/2017). The study with animals followed Spanish and European Union guidelines for animal experimentation (RD 1201/05, RD 53/2013 and 86/609/CEE) and was approved by the Bioethics Committee of the University of Salamanca and Conserjería de Agricultura y Ganadería de la Junta de Castilla y León (registration number 359).

ACKNOWLEDGEMENTS

We thank the Radioactive Isotopes and Radioprotection Services for mouse irradiation, and the cell separation, experimental animal and transgenic facilities of NUCLEUS, University of Salamanca, for carrying out the FACS and animal assays.

FUNDING

This work was supported by the Research Support Platform of the University of Salamanca (NUCLEUS), Instituto Carlos III (ISCIII) PI17/01895 (ISCIII-FEDER), Novartis Farmaceutica S.A., a predoctoral grant from University of Salamanca-Banco Santander, and Jabones Solidarios para Daniel from the Bomberos Ayudan Association.

AUTHOR CONTRIBUTIONS

Conceptualization: Manuel Sánchez-Martín.
Design and Investigation: Ignacio García-Tuñón, Manuel Sánchez-Martín.
Data curation: Elena Vuelta, Ignacio García-Tuñón.
Statistical analysis: Elena Vuelta, Ignacio García-Tuñón.
Methodology: Elena Vuelta, Ignacio García-Tuñón, Manuel Sánchez-Martín.
Animal care: Lucía Méndez, Patricia Hernández-Carabias, José Luis Ordóñez.
Resources: Lucía Méndez, Patricia Hernández-Carabias, José Luis Ordoñez, Verónica Alonso-Pérez.
Human samples and clinical data: Raquel Saldaña, Julián Sevilla, Fermín Sánchez-Guijo, Sandra Muntión, Jesús María Hernández-Rivas.
Funding acquisition: Jesús María Hernández-Rivas, Ignacio García-Tuñón, Manuel Sánchez-Martín.
Project administration: Ignacio García-Tuñón, Manuel Sánchez-Martín.
Supervision: Ignacio García-Tuñón, Manuel Sánchez-Martín
Figures: Elena Vuelta, Ignacio García-Tuñón, Manuel Sánchez-Martín
Writing – original draft: Ignacio García-Tuñón, Manuel Sánchez-Martín.

Competing interests

The authors have declared that they have no competing interests.

REFERENCES

1. Nowell PC. The minute chromosome (Phl) in chronic granulocytic leukemia. Blut [Internet]. 1962;8:65–6. Available from: https://www.ncbi.nlm.nih.gov/pubmed/14480647
2. Rowley JD. Letter: A new consistent chromosomal abnormality in chronic myelogenous leukaemia identified by quinacrine fluorescence and Giemsa staining. Nature [Internet]. 1973;243(5405):290–3. Available from: https://www.ncbi.nlm.nih.gov/pubmed/4126434
3. Wang Y, Wu N, Liu D, Jin Y. Recurrent Fusion Genes in Leukemia: An Attractive Target for Diagnosis and Treatment. Curr Genomics. 2017 Oct;18(5):378–84.
4. Ben-Neriah Y, Daley GQ, Mes-Masson AM, Witte ON, Baltimore D. The chronic myelogenous leukemia-specific P210 protein is the product of the bcr/abl hybrid gene. Science (80-) [Internet]. 1986;233(4760):212–4. Available from: https://www.ncbi.nlm.nih.gov/pubmed/3460176
5. Janossy G, Roberts M, Greaves MF. Target cell in chronic myeloid leukaemia and its relationship to acute lymphoid leukaemia. Lancet (London, England). 1976 Nov;2(7994):1058–61.
6. Zhou H, Xu R. Leukemia stem cells: the root of chronic myeloid leukemia. Protein Cell. 2015 Jun;6(6):403–12.
7. Tauchi T, Boswell HS, Leibowitz D, Broxmeyer HE. Coupling between p210bcr-abl and Shc and Grb2 adaptor proteins in hematopoietic cells permits growth factor receptor-independent link to ras activation pathway. J Exp Med. 1994 Jan;179(1):167–75.
8. Kabarowski JH, Witte ON. Consequences of BCR-ABL expression within the hematopoietic stem cell in chronic myeloid leukemia. Stem Cells. 2000;18(6):399–408.
9. Konopka JB, Watanabe SM, Witte ON. An alteration of the human c-abl protein in K562 leukemia cells unmasks associated tyrosine kinase activity. Cell. 1984 Jul;37(3):1035–42.
10. Konopka JB, Watanabe SM, Singer JW, Collins SJ, Witte ON. Cell lines and clinical isolates derived from Ph1-positive chronic myelogenous leukemia patients express c-abl proteins with a common structural alteration. Proc Natl Acad Sci U S A. 1985 Mar;82(6):1810–4.
11. Braun TP, Eide CA, Druker BJ. Response and Resistance to BCR-ABL1-Targeted Therapies. Cancer Cell. 2020 Apr;37(4):530–42.
12. McWhirter JR, Galasso DL, Wang JY. A coiled-coil oligomerization domain of Bcr is essential for the transforming function of Bcr-Abl oncoproteins. Mol Cell Biol. 1993 Dec;13(12):7587–95.
13. Muller AJ, Young JC, Pendergast AM, Pondel M, Landau NR, Littman DR, et al. BCR first exon sequences specifically activate the BCR/ABL tyrosine kinase oncogene of Philadelphia chromosome-positive human leukemias. Mol Cell Biol. 1991 Apr;11(4):1785–92.
14. Pendergast AM, Gishizky ML, Havlik MH, Witte ON. SH1 domain autophosphorylation of P210 BCR/ABL is required for transformation but not growth factor independence. Mol Cell Biol. 1993 Mar;13(3):1728–36.
15. Ma G, Lu D, Wu Y, Liu J, Arlinghaus RB. Bcr phosphorylated on tyrosine 177 binds Grb2. Oncogene. 1997 May;14(19):2367–72.
16. Reuther GW, Fu H, Cripe LD, Collier RJ, Pendergast AM. Association of the

protein kinases c-Bcr and Bcr-Abl with proteins of the 14-3-3 family. Science. 1994 Oct;266(5182):129–33.

17. Egan SE, Giddings BW, Brooks MW, Buday L, Sizeland AM, Weinberg RA. Association of Sos Ras exchange protein with Grb2 is implicated in tyrosine kinase signal transduction and transformation. Nature. 1993 May;363(6424):45–51.
18. Shuai K, Halpern J, ten Hoeve J, Rao X, Sawyers CL. Constitutive activation of STAT5 by the BCR-ABL oncogene in chronic myelogenous leukemia. Oncogene. 1996 Jul;13(2):247–54.
19. Ilaria RLJ, Van Etten RA. P210 and P190(BCR/ABL) induce the tyrosine phosphorylation and DNA binding activity of multiple specific STAT family members. J Biol Chem. 1996 Dec;271(49):31704–10.
20. Carlesso N, Frank DA, Griffin JD. Tyrosyl phosphorylation and DNA binding activity of signal transducers and activators of transcription (STAT) proteins in hematopoietic cell lines transformed by Bcr/Abl. J Exp Med. 1996 Mar;183(3):811–20.
21. Frank DA, Varticovski L. BCR/abl leads to the constitutive activation of Stat proteins, and shares an epitope with tyrosine phosphorylated Stats. Leukemia. 1996 Nov;10(11):1724–30.
22. Wong S, Witte ON. The BCR-ABL story: bench to bedside and back. Annu Rev Immunol. 2004;22:247–306.
23. Kantarjian H, O'Brien S, Jabbour E, Garcia-Manero G, Quintas-Cardama A, Shan J, et al. Improved survival in chronic myeloid leukemia since the introduction of imatinib therapy: a single-institution historical experience. Blood. 2012 Mar;119(9):1981–7.
24. Chereda B, Melo J V. Natural course and biology of CML. Ann Hematol. 2015 Apr;94 Suppl 2:S107-21.
25. Deininger M, O'Brien SG, Guilhot F, Goldman JM, Hochhaus A, Hughes TP, et al. International Randomized Study of Interferon Vs STI571 (IRIS) 8-Year Follow up: Sustained Survival and Low Risk for Progression or Events in Patients with Newly Diagnosed Chronic Myeloid Leukemia in Chronic Phase (CML-CP) Treated with Imatinib. Blood [Internet]. 2009 Nov 20;114(22):1126. Available from: https://doi.org/10.1182/blood.V114.22.1126.1126
26. Bower H, Björkholm M, Dickman PW, Höglund M, Lambert PC, Andersson TM-L. Life Expectancy of Patients With Chronic Myeloid Leukemia Approaches the Life Expectancy of the General Population. J Clin Oncol Off J Am Soc Clin Oncol. 2016 Aug;34(24):2851–7.
27. Chandra HS, Heisterkamp NC, Hungerford A, Morrissette JJD, Nowell PC, Rowley JD, et al. Philadelphia Chromosome Symposium: commemoration of the 50th anniversary of the discovery of the Ph chromosome. Vol. 204, Cancer genetics. United States; 2011. p. 171–9.
28. Milojkovic D, Apperley J. Mechanisms of Resistance to Imatinib and Second-Generation Tyrosine Inhibitors in Chronic Myeloid Leukemia. Clin Cancer Res. 2009 Dec;15(24):7519–27.
29. Graham SM, Jorgensen HG, Allan E, Pearson C, Alcorn MJ, Richmond L, et al. Primitive, quiescent, Philadelphia-positive stem cells from patients with chronic myeloid leukemia are insensitive to STI571 in vitro. Blood. 2002/01/05. 2002;99(1):319–25.
30. Jinek M, Chylinski K, Fonfara I, Hauer M, Doudna JA, Charpentier E. A programmable dual-RNA-guided DNA endonuclease in adaptive bacterial

immunity. Science (80-) [Internet]. 2012;337(6096):816–21. Available from: https://www.ncbi.nlm.nih.gov/pubmed/22745249

31. Mojica FJM, Montoliu L. On the Origin of CRISPR-Cas Technology: From Prokaryotes to Mammals. Trends Microbiol [Internet]. 2016;24(10):811–20. Available from: https://www.ncbi.nlm.nih.gov/pubmed/27401123
32. Wassef M, Luscan A, Battistella A, Le Corre S, Li H, Wallace MR, et al. Versatile and precise gene-targeting strategies for functional studies in mammalian cell lines. Methods [Internet]. 2017;121–122:45–54. Available from: https://www.ncbi.nlm.nih.gov/pubmed/28499832
33. Garcia-Tuñon I, Hernandez-Sanchez M, Ordonez JL, Alonso-Perez V, Alamo-Quijada M, Benito R, et al. The CRISPR/Cas9 system efficiently reverts the tumorigenic ability of BCR/ABL in vitro and in a xenograft model of chronic myeloid leukemia. Oncotarget [Internet]. 2017; Available from: https://www.ncbi.nlm.nih.gov/pubmed/28212528
34. Garcia-Tuñon I, Alonso-Perez V, Vuelta E, Perez-Ramos S, Herrero M, Mendez L, et al. Splice donor site sgRNAs enhance CRISPR/Cas9-mediated knockout efficiency. PLoS One. 2019;14(5):e0216674.
35. García-Tuñon I, Vuelta E, Pérez-Ramos S, Hernández-Rivas JM, Méndez L, Herrero M, et al. CRISPR-ERA for Switching Off (Onco) Genes. 2016;
36. Honda H, Oda H, Suzuki T, Takahashi T, Witte ON, Ozawa K, et al. Development of acute lymphoblastic leukemia and myeloproliferative disorder in transgenic mice expressing p210bcr/abl: a novel transgenic model for human Ph1-positive leukemias. Blood. 1998 Mar;91(6):2067–75.
37. Apperley JF. Chronic myeloid leukaemia. Lancet (London, England). 2015 Apr;385(9976):1447–59.
38. Ankathil R, Azlan H, Dzarr AA, Baba AA. Pharmacogenetics and the treatment of chronic myeloid leukemia: how relevant clinically? An update. Pharmacogenomics. 2018/03/24. 2018;19(5):393–475.
39. Shultz LD, Lyons BL, Burzenski LM, Gott B, Chen X, Chaleff S, et al. Human lymphoid and myeloid cell development in NOD/LtSz-scid IL2R gamma null mice engrafted with mobilized human hemopoietic stem cells. J Immunol. 2005 May;174(10):6477–89.
40. Ito M, Hiramatsu H, Kobayashi K, Suzue K, Kawahata M, Hioki K, et al. NOD/SCID/gamma(c)(null) mouse: an excellent recipient mouse model for engraftment of human cells. Blood. 2002 Nov;100(9):3175–82.
41. McDermott SP, Eppert K, Lechman ER, Doedens M, Dick JE. Comparison of human cord blood engraftment between immunocompromised mouse strains. Blood. 2010 Jul;116(2):193–200.
42. Groffen J, Stephenson JR, Heisterkamp N, de Klein A, Bartram CR, Grosveld G. Philadelphia chromosomal breakpoints are clustered within a limited region, bcr, on chromosome 22. Cell. 1984 Jan;36(1):93–9.
43. Heisterkamp N, Stam K, Groffen J, de Klein A, Grosveld G. Structural organization of the bcr gene and its role in the Ph' translocation. Nature. 1985 Jun;315(6022):758–61.
44. Shtivelman E, Lifshitz B, Gale RP, Canaani E. Fused transcript of abl and bcr genes in chronic myelogenous leukaemia. Nature. 1985 Jun;315(6020):550–4.
45. Stam K, Heisterkamp N, Grosveld G, de Klein A, Verma RS, Coleman M, et al. Evidence of a new chimeric bcr/c-abl mRNA in patients with chronic myelocytic leukemia and the Philadelphia chromosome. N Engl J Med. 1985 Dec;313(23):1429–33.

46. Palacios R, Steinmetz M. Il-3-dependent mouse clones that express B-220 surface antigen, contain Ig genes in germ-line configuration, and generate B lymphocytes in vivo. Cell. 1985/07/01. 1985;41(3):727–34.
47. Daley GQ, Baltimore D. Transformation of an interleukin 3-dependent hematopoietic cell line by the chronic myelogenous leukemia-specific P210bcr/abl protein. Proc Natl Acad Sci U S A. 1988/12/01. 1988;85(23):9312–6.
48. Schultze N, Burki Y, Lang Y, Certa U, Bluethmann H. Efficient control of gene expression by single step integration of the tetracycline system in transgenic mice. Nat Biotechnol. 1996/04/01. 1996;14(4):499–503.
49. Perez-Caro M, Gutierrez-Cianca N, Gonzalez-Herrero I, Lopez-Hernandez I, Flores T, Orfao A, et al. Sustained leukaemic phenotype after inactivation of BCR-ABLp190 in mice. Oncogene. 2006/09/20. 2007;26(12):1702–13.
50. Herrero AB, San Miguel J, Gutierrez NC. Deregulation of DNA double-strand break repair in multiple myeloma: implications for genome stability. PLoS One. 2015;10(3):e0121581.

Figure 1

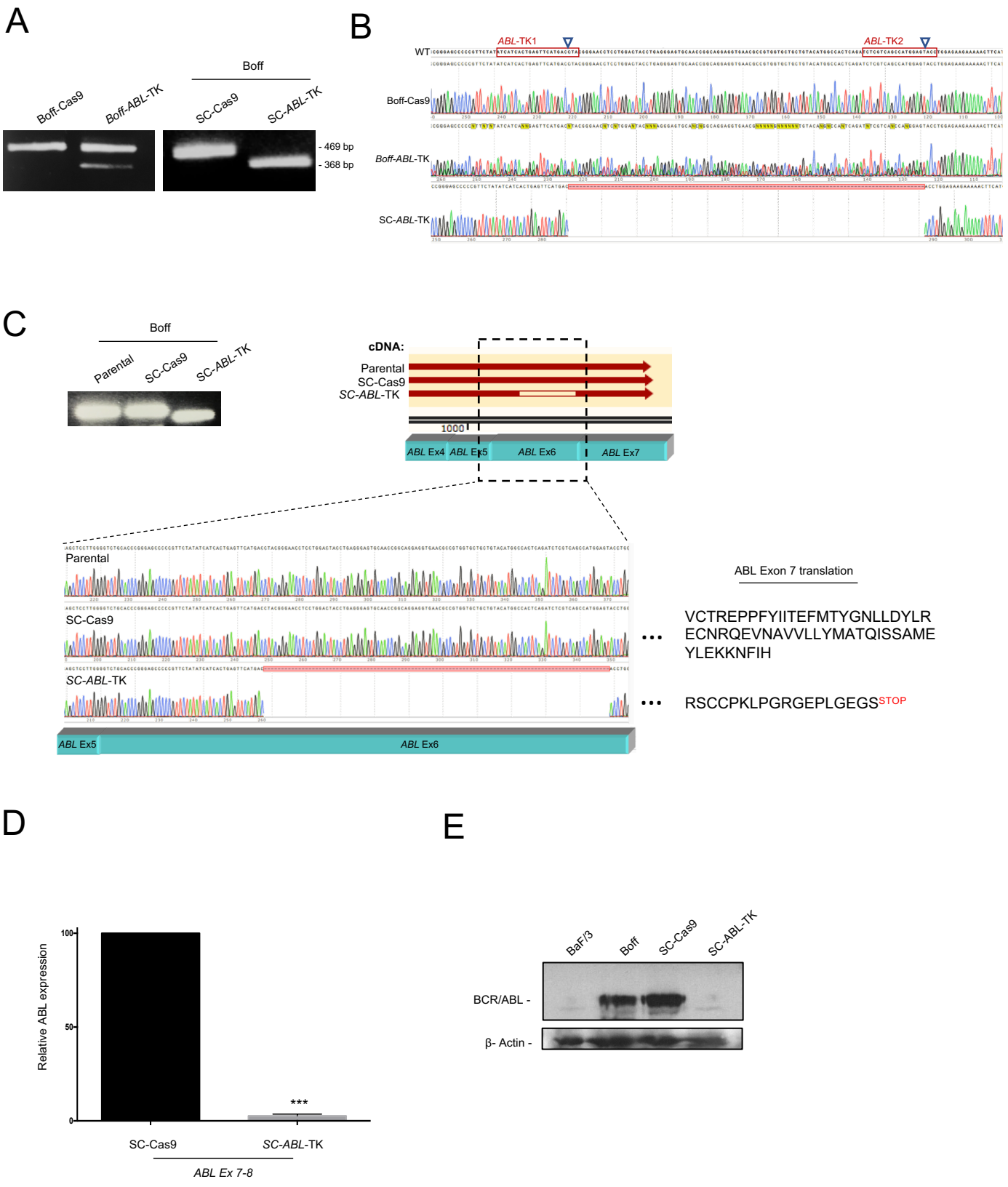
A
Boff
Boff-Cas9
Boff-ABL-TK
SC-Cas9
SC-ABL-TK
- 469 bp
- 368 bp
B
ABL-TK1
ABL-TK2
WT
Boff-Cas9
Boff-ABL-TK
SC-ABL-TK
C
Boff
Parental
SC-Cas9
SC-ABL-TK
cDNA:
Parental
SC-Cas9
SC-ABL-TK
1000
ABL Ex4
ABL Ex5
ABL Ex6
ABL Ex7
Parental
SC-Cas9
SC-ABL-TK
ABL Ex5
ABL Ex6
ABL Exon 7 translation
VCTREPPFYIITEFMTYGNLLDYLR
ECNRQEVNAVVLLYMATQISSAME
YLEKKNFIH
RSCCPKLPGRGEPLGEGS STOP
D
Relative ABL expression
100
50
0
***
SC-Cas9
SC-ABL-TK
ABL Ex 7-8
E
BaF/3
Boff
SC-Cas9
SC-ABL-TK
BCR/ABL -
β- Actin -

Figure 2

A


K562
Cas9
ABL-TK
- 473 bp
- 372 bp
ABL-TK1
ABL-TK2
K562-ABL-TK

B

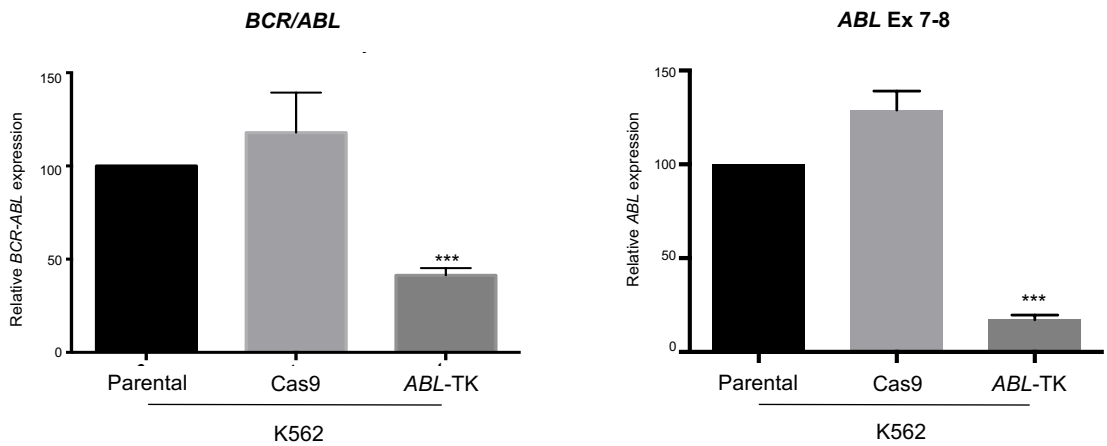
BCR/ABL
Relative BCR-ABL expression
150
100
50
0
***
Parental
Cas9
ABL-TK
K562
ABL Ex 7-8
Relative ABL expression
150
100
50
0
***
Parental
Cas9
ABL-TK
K562

c

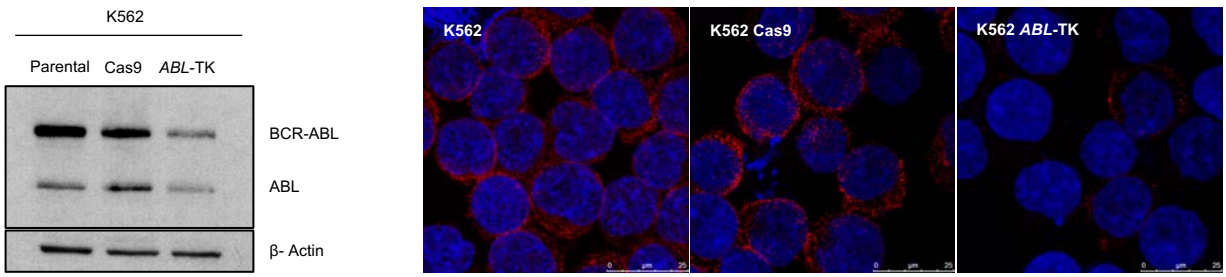
K562
Parental
Cas9
ABL-TK
BCR-ABL
ABL
β- Actin
K562
K562 Cas9
K562 ABL-TK

Figure 3

A

B

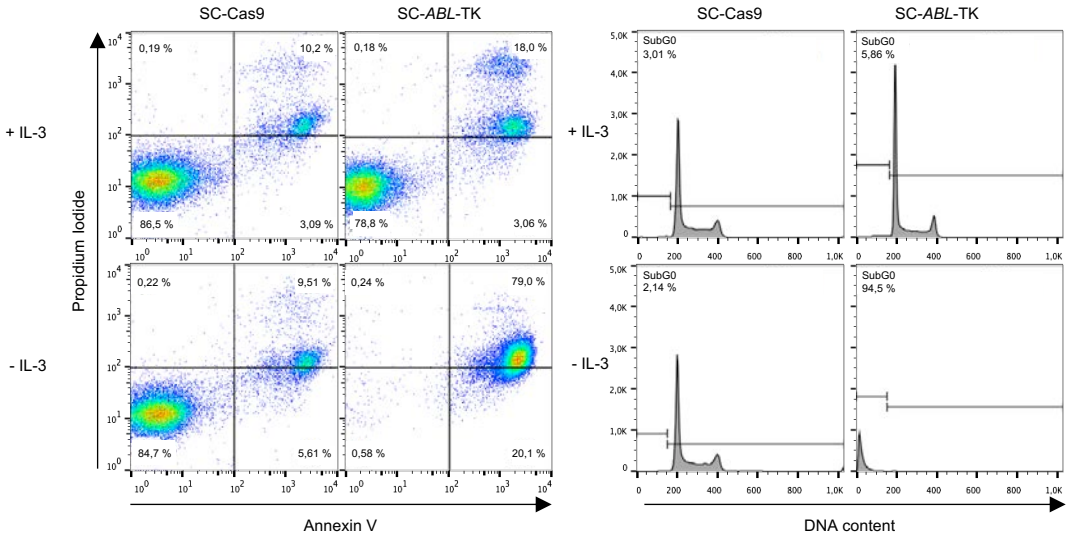
SC-Cas9
SC-ABL-TK
+ IL-3
- IL-3
Propidium Iodide
Annexin V
0,19 %
10,2 %
86,5 %
3,09 %
0,18 %
18,0 %
78,8 %
3,06 %
0,22 %
9,51 %
84,7 %
5,61 %
0,24 %
79,0 %
0,58 %
20,1 %
SubG0
3,01 %
SubG0
5,86 %
SubG0
2,14 %
SubG0
94,5 %
DNA content

Figure 4

A

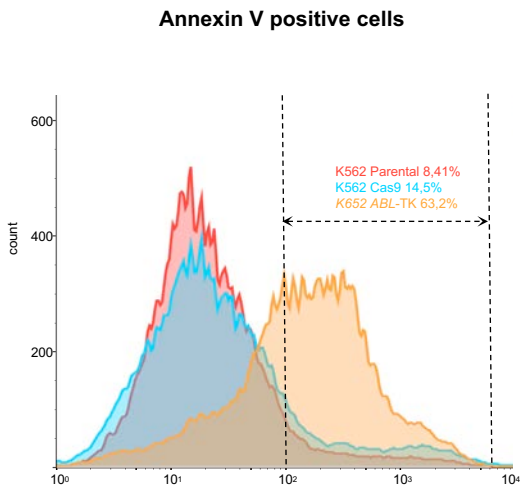
Annexin V positive cells
600
400
200
count
K562 Parental 8,41%
K562 Cas9 14,5%
K652 ABL-TK 63,2%
10⁰
10¹
10²
10³
10⁴

B

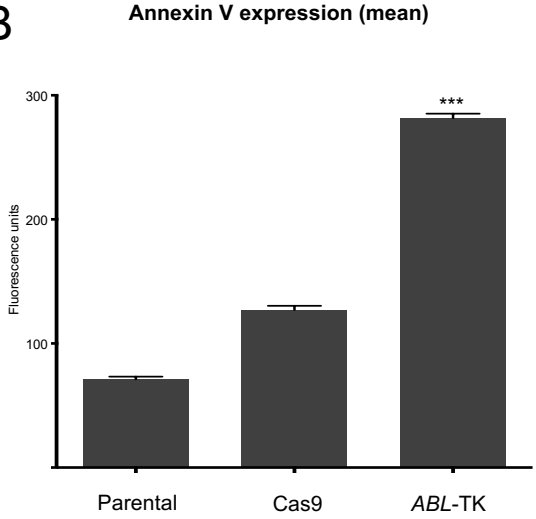
Annexin V expression (mean)
300
200
100
Fluorescence units
***
Parental
Cas9
ABL-TK

C

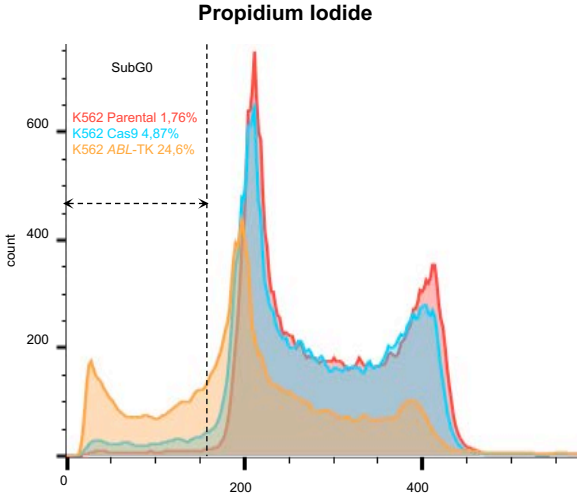
Propidium Iodide
SubG0
K562 Parental 1,76%
K562 Cas9 4,87%
K562 ABL-TK 24,6%
600
400
200
count
0
200
400

Figure 5

A

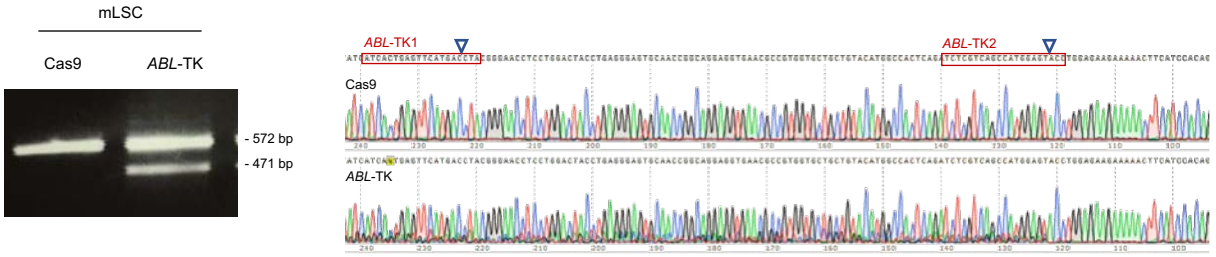
mLSC
Cas9
ABL-TK
- 572 bp
- 471 bp
ABL-TK1
ABL-TK2
Cas9
ABL-TK

B

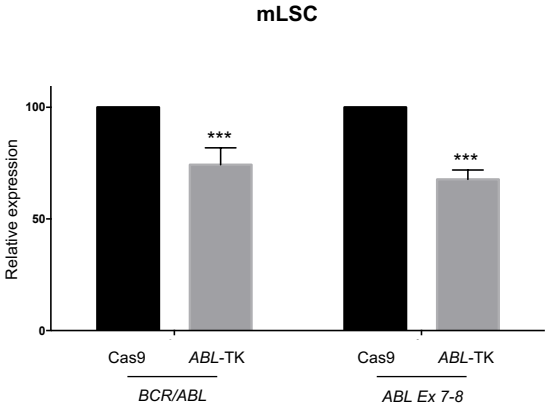
mLSC
Relative expression
100
50
0
***
***
Cas9
ABL-TK
Cas9
ABL-TK
BCR/ABL
ABL Ex 7-8

C

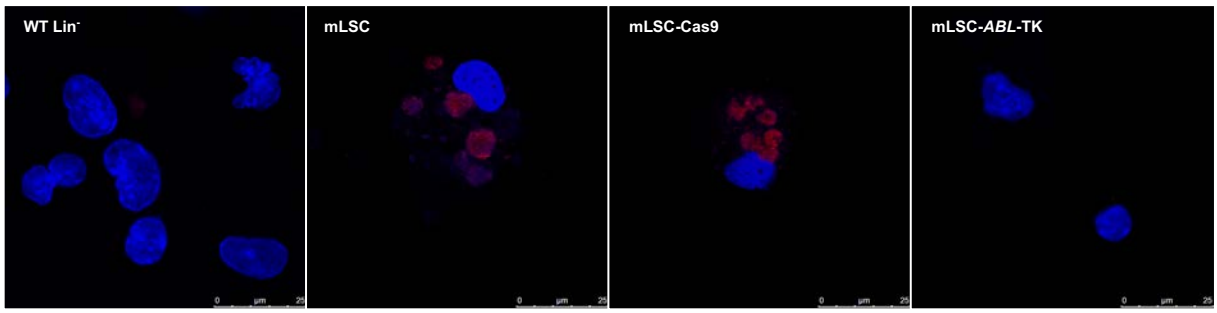
WT Lin-
mLSC
mLSC-Cas9
mLSC-ABL-TK

Figure 6

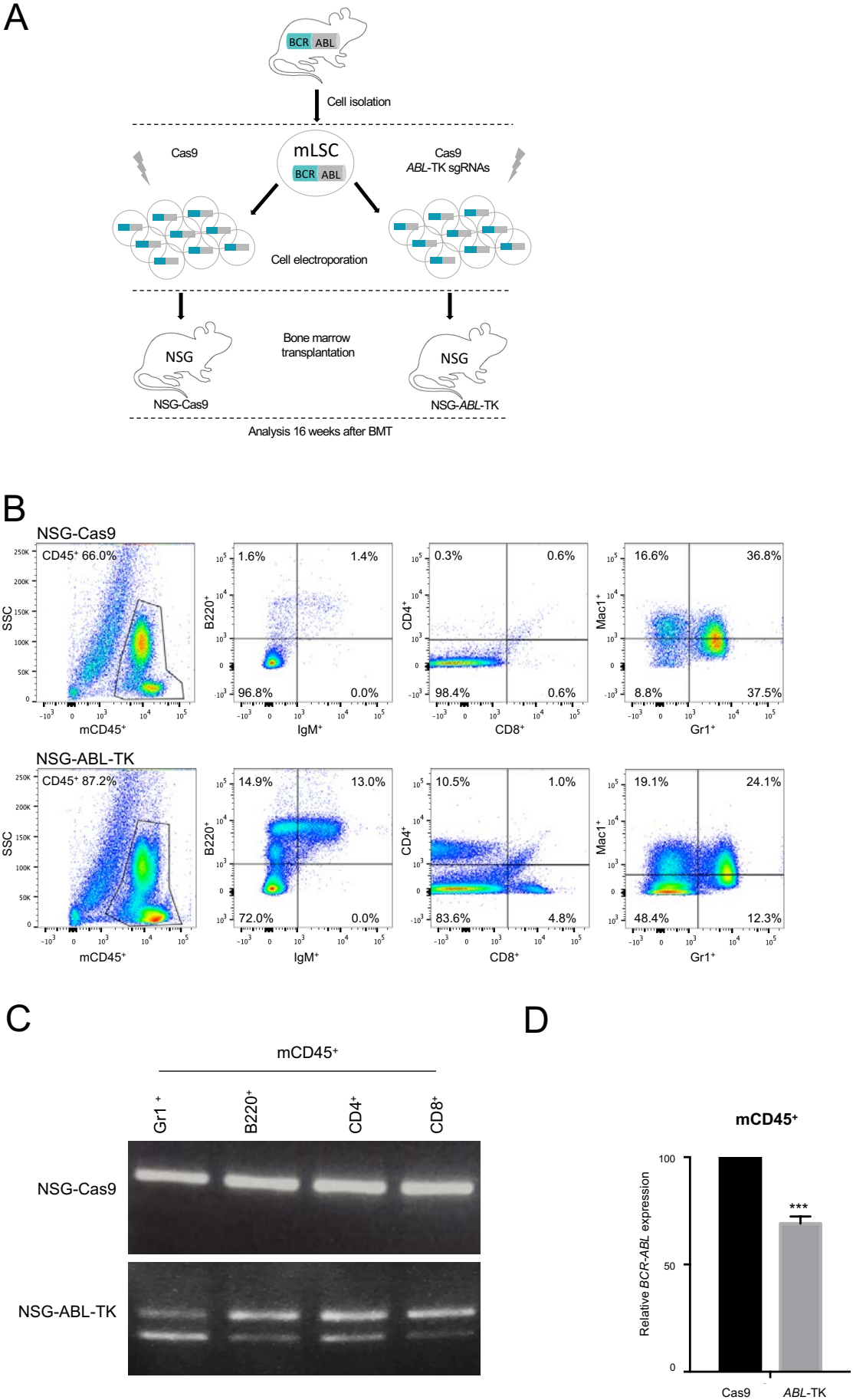
A
BCR ABL
Cell isolation
mLSC
BCR ABL
Cas9
Cas9
ABL-TK sgRNAs
Cell electroporation
Bone marrow
transplantation
NSG
NSG
NSG-Cas9
NSG-ABL-TK
Analysis 16 weeks after BMT
B
NSG-Cas9
CD45+ 66.0%
SSC
mCD45+
1.6%
1.4%
96.8%
0.0%
B220+
IgM+
0.3%
0.6%
98.4%
0.6%
CD4+
CD8+
16.6%
36.8%
8.8%
37.5%
Mac1+
Gr1+
NSG-ABL-TK
CD45+ 87.2%
SSC
mCD45+
14.9%
13.0%
72.0%
0.0%
B220+
IgM+
10.5%
1.0%
83.6%
4.8%
CD4+
CD8+
19.1%
24.1%
48.4%
12.3%
Mac1+
Gr1+
C
mCD45+
Gr1+
B220+
CD4+
CD8+
NSG-Cas9
NSG-ABL-TK
D
mCD45+
Relative BCR-ABL expression
100
50
0
***
Cas9
ABL-TK
BCR/ABL

Figure 7

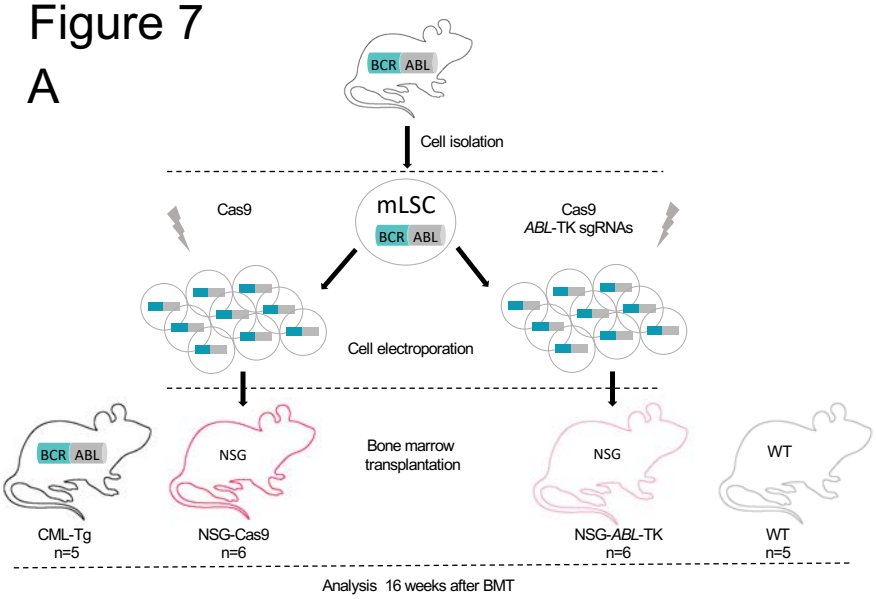
A
BCR ABL
Cell isolation
mLSC
BCR ABL
Cas9
Cas9
ABL-TK sgRNAs
Cell electroporation
BCR ABL
NSG
Bone marrow
transplantation
NSG
WT
CML-Tg
n=5
NSG-Cas9
n=6
NSG-ABL-TK
n=6
WT
n=5
Analysis 16 weeks after BMT

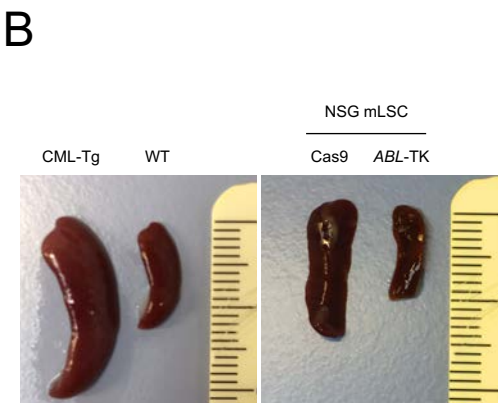
B
NSG mLSC
CML-Tg
WT
Cas9
ABL-TK

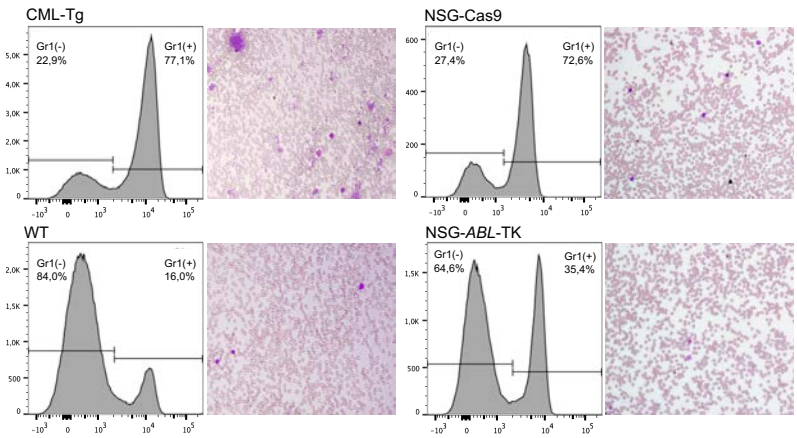
C
CML-Tg
Gr1(-)
22,9%
Gr1(+)
77,1%
NSG-Cas9
Gr1(-)
27,4%
Gr1(+)
72,6%
WT
Gr1(-)
84,0%
Gr1(+)
16,0%
NSG-ABL-TK
Gr1(-)
64,6%
Gr1(+)
35,4%

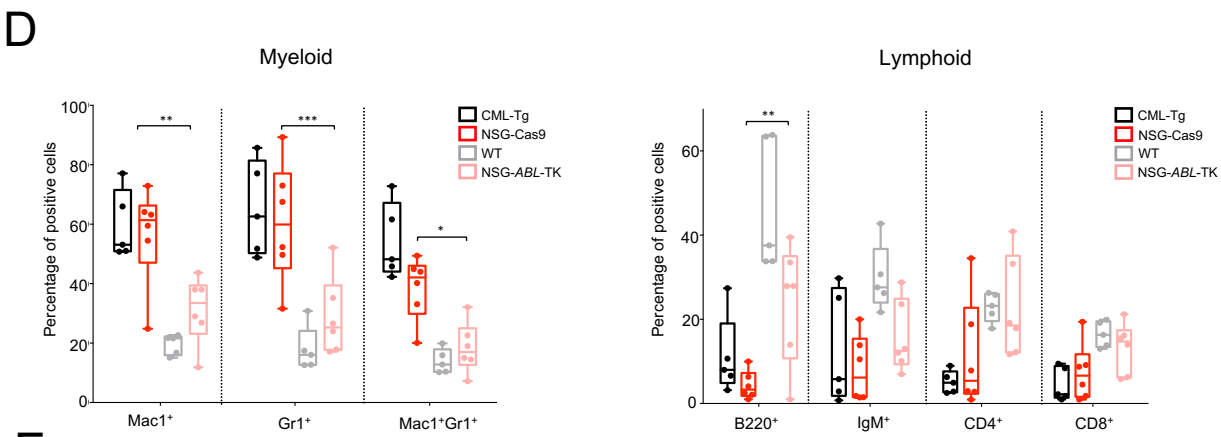
D
Myeloid
Lymphoid
Percentage of positive cells
CML-Tg
NSG-Cas9
WT
NSG-ABL-TK
Mac1+
Gr1+
Mac1+Gr1+
B220+
IgM+
CD4+
CD8+

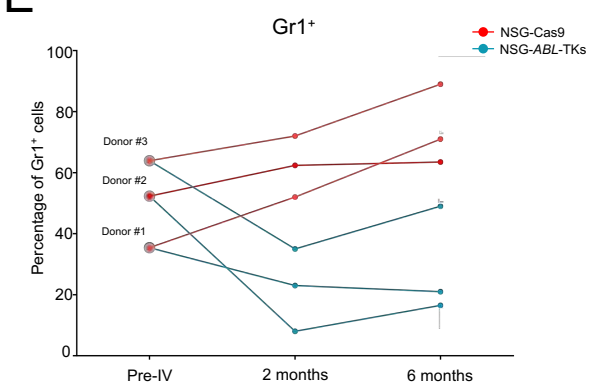
E
Gr1+
NSG-Cas9
NSG-ABL-TKs
Percentage of Gr1+ cells
Donor #3
Donor #2
Donor #1
Pre-IV
2 months
6 months

Figure 8

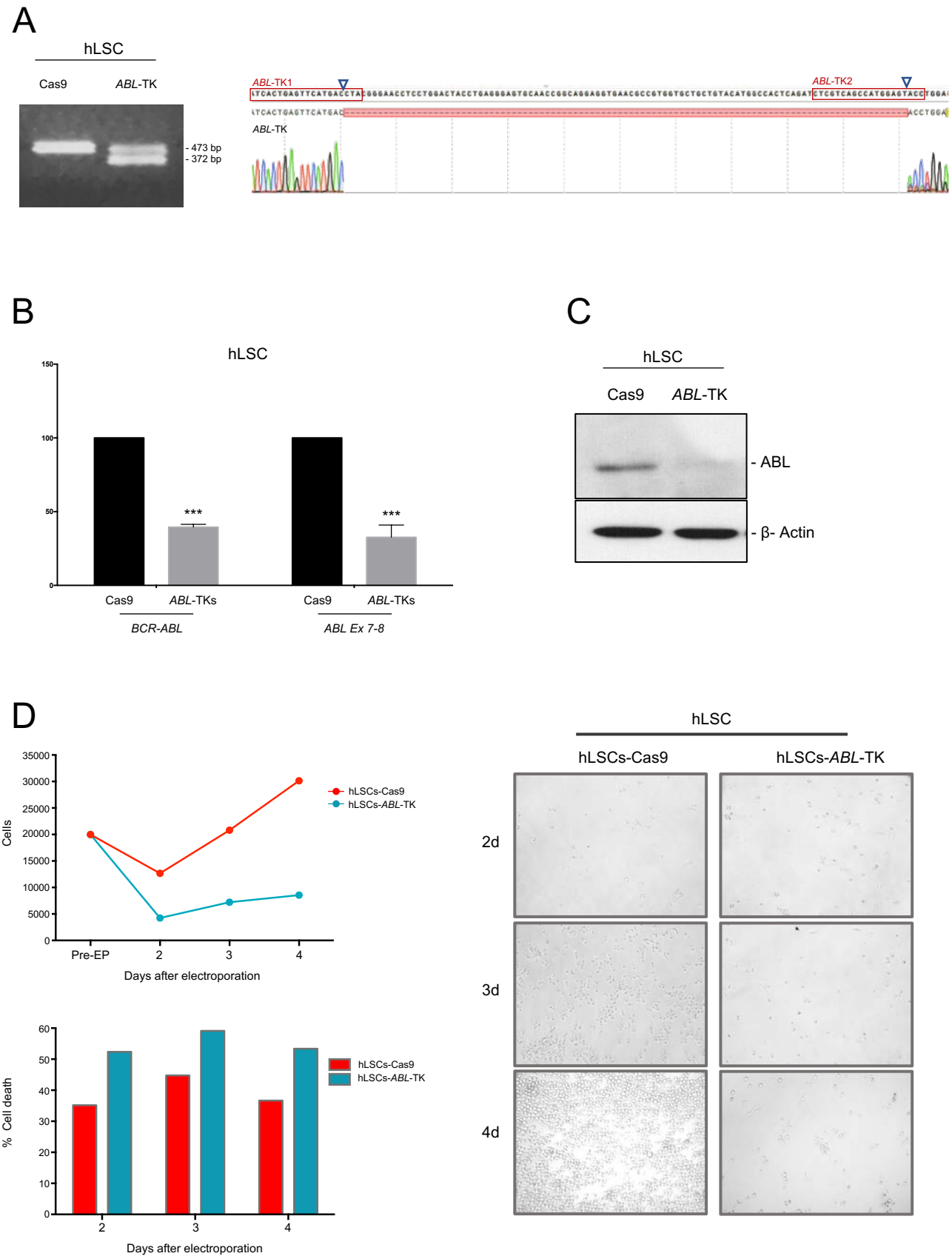
A
hLSC
Cas9
ABL-TK
- 473 bp
- 372 bp
ABL-TK1
ABL-TK2
ABL-TK
B
hLSC
150
100
50
0
***
***
Cas9
ABL-TKs
Cas9
ABL-TKs
BCR-ABL
ABL Ex 7-8
C
hLSC
Cas9
ABL-TK
- ABL
- β- Actin
D
35000
30000
25000
20000
15000
10000
5000
0
Cells
hLSCs-Cas9
hLSCs-ABL-TK
Pre-EP
2
3
4
Days after electroporation
60
50
40
30
20
10
0
% Cell death
hLSCs-Cas9
hLSCs-ABL-TK
2
3
4
Days after electroporation
hLSC
hLSCs-Cas9
hLSCs-ABL-TK
2d
3d
4d

Figure 9

A

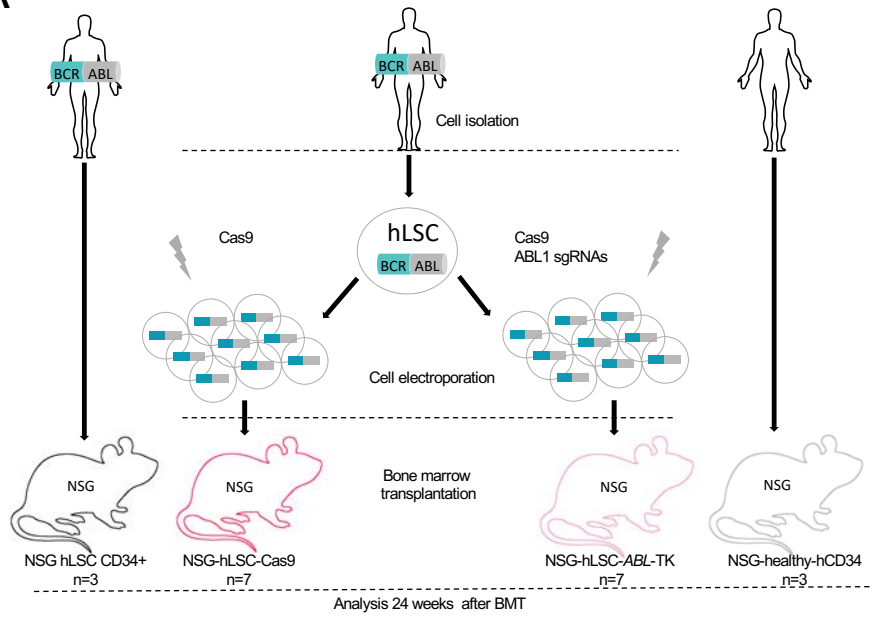
BCR ABL
BCR ABL
Cell isolation
hLSC
BCR ABL
Cas9
Cas9
ABL1 sgRNAs
Cell electroporation
NSG
NSG
Bone marrow
transplantation
NSG
NSG
NSG hLSC CD34+
n=3
NSG-hLSC-Cas9
n=7
NSG-hLSC-*ABL*-TK
n=7
NSG-healthy-hCD34
n=3
Analysis 24 weeks after BMT

Figure 9

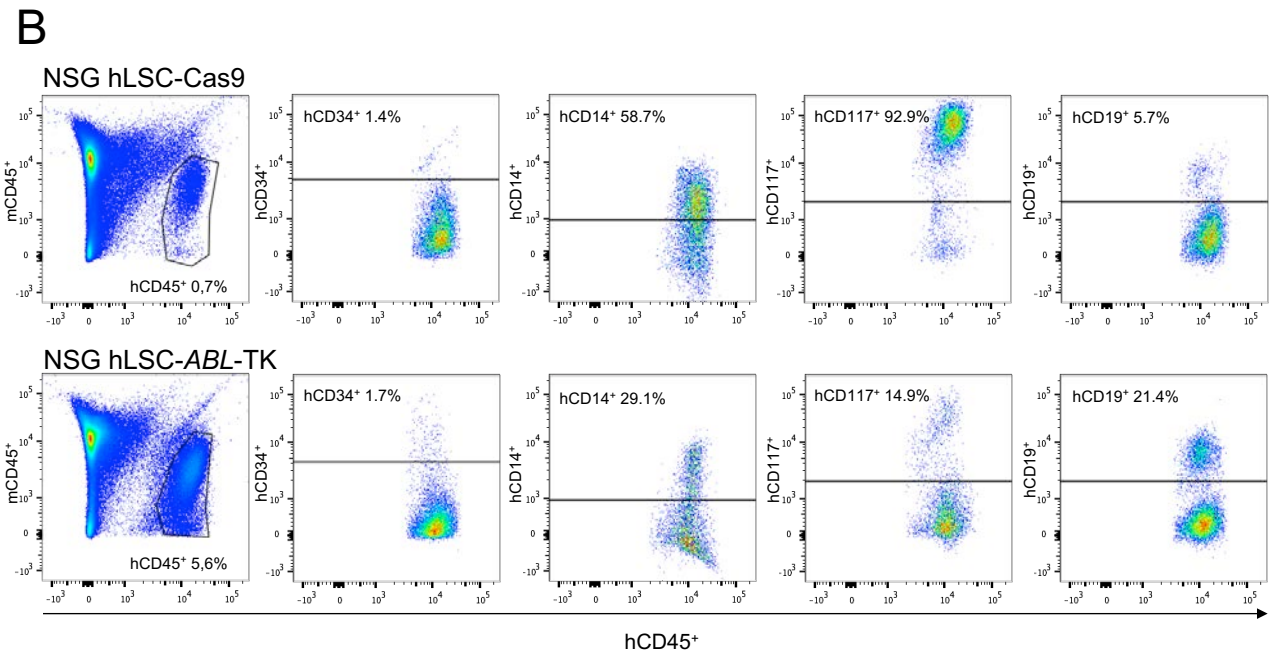
B
NSG hLSC-Cas9
mCD45+
hCD45+ 0,7%
hCD34+ 1.4%
hCD14+ 58.7%
hCD117+ 92.9%
hCD19+ 5.7%
NSG hLSC-ABL-TK
hCD45+ 5,6%
hCD34+ 1.7%
hCD14+ 29.1%
hCD117+ 14.9%
hCD19+ 21.4%
hCD45+

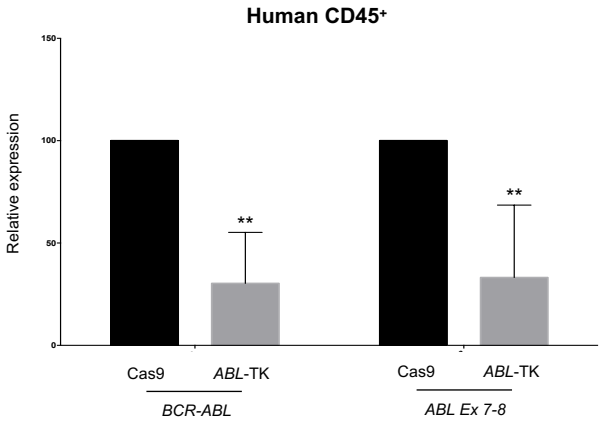
C
Human CD45+
Relative expression
150
100
50
0
**
**
Cas9
ABL-TK
Cas9
ABL-TK
BCR-ABL
ABL Ex 7-8

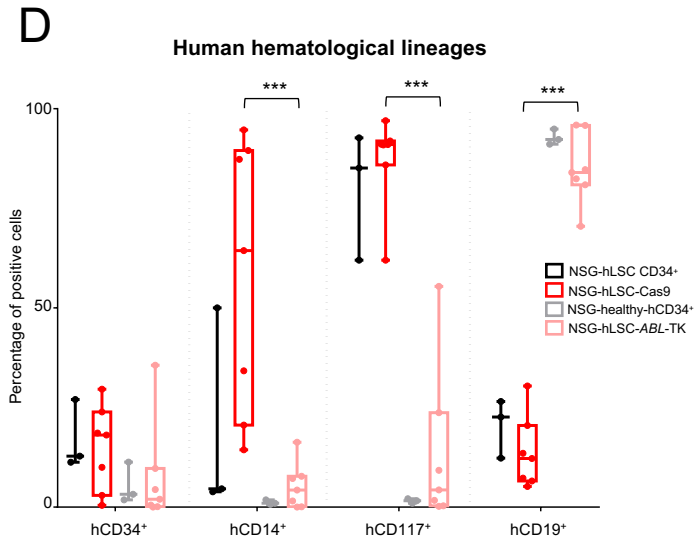
D
Human hematological lineages
Percentage of positive cells
100
50
0
***
***
***
NSG-hLSC CD34+
NSG-hLSC-Cas9
NSG-healthy-hCD34+
NSG-hLSC-ABL-TK
hCD34+
hCD14+
hCD117+
hCD19+

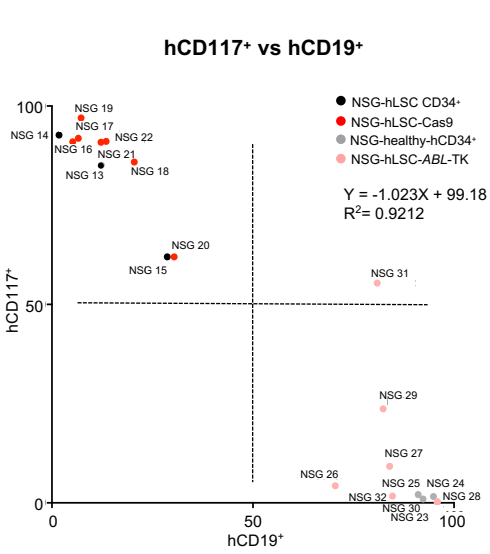
E
hCD117+ vs hCD19+
NSG-hLSC CD34+
NSG-hLSC-Cas9
NSG-healthy-hCD34+
NSG-hLSC-ABL-TK
Y = -1.023X + 99.18
R2= 0.9212
hCD117+
hCD19+
100
50
0
50
100
NSG 19
NSG 17
NSG 14
NSG 22
NSG 16
NSG 21
NSG 13
NSG 18
NSG 20
NSG 15
NSG 31
NSG 29
NSG 27
NSG 26
NSG 25
NSG 24
NSG 32
NSG 28
NSG 30
NSG 23

Figure S1

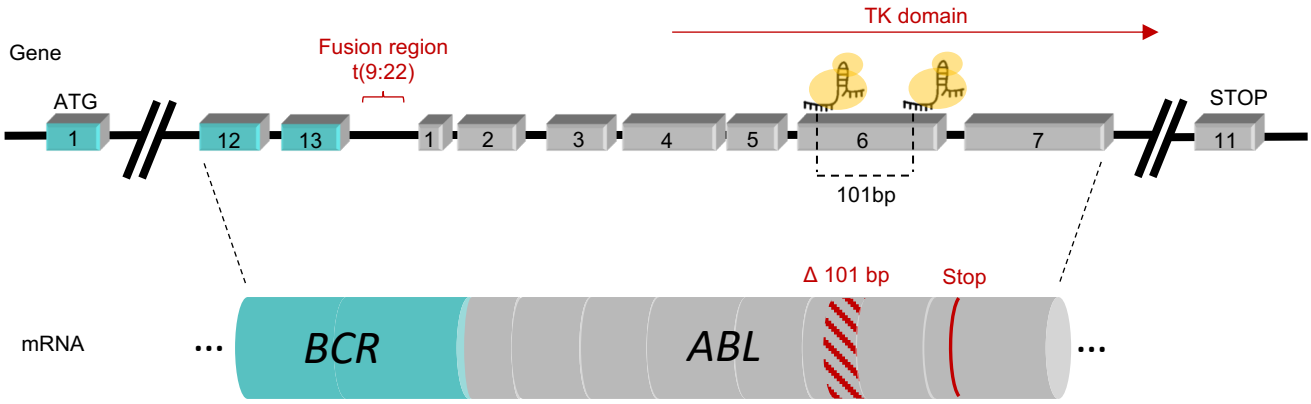
Gene
ATG
Fusion region
t(9:22)
TK domain
STOP
1
12
13
1
2
3
4
5
6
7
11
101bp
mRNA
BCR
ABL
Δ 101 bp
Stop

Figure legends

Figure 1.- Functional analysis of the CRISPR/Cas9 deletion system in the Boff-p210 cell line. (A) PCR amplification of ABL exon 6 in Boff-p210 cells electroporated with solely Cas9 (Boff-Cas9), with Cas9 and both sgRNAs (Boff-*ABL*-TK), and in single-cell clones derived (SC-Cas9 and SC-*ABL*-TK). (B) Sanger sequencing of the amplified region of *ABL* exon 6. (C) RT-PCR of *ABL* exon 6 showing a smaller mRNA transcript in SC-*ABL*-TK than in control cells (parental and SC-Cas9). The 101-bp deletion was confirmed by Sanger sequencing in SC-*ABL*-TKs. *In silico* analysis shows this deletion generates a premature stop codon in *ABL* exon 7. (D) Quantitative PCR of ABL expression in Boff-p210 single-edited cell-derived clones (SC) at the exon 7-8 level. (mean ± SEM; *** $p<0.001$). (E) Western blot of BCR-ABL in Baf/3, Boff, and SC cells.

Figure 2.- Functional analysis of the CRISPR/Cas9 deletion system in the K562 human cell line. (A) PCR amplification of ABL exon 6 in K562 cells electroporated with Cas9 nuclease (K562-Cas9) and with Cas9 joined to both sgRNAs (K562-*ABL*-TKs). Sanger sequencing of the amplified region revealed a 101-bp deletion between the expected cleavage points. (B) Quantitative PCR of *BCR/ABL* (left) and *ABL* (right) mRNA in K562 (parental), K562-Cas9 and K562-*ABL*-TK (mean ± SEM; *** $p<0.001$). (C) Western blot of ABL protein in parental, K562-Cas9 and K562-*ABL*-TK (left). These results were corroborated by immunocytochemistry (right).

Figure 3.- Functional analysis of CRISPR/Cas9 deletion system in a CML murine cell line. (A) Annexin-V cell apoptosis assay of SC cells in the presence or absence of IL-3. (B) Cell cycle assay of SC cells in the presence or absence of IL-3.

Figure 4.- Analysis of cell viability in the CRISPR/Cas9-deletion system in a CML human cell line. (A) Annexin-V cell apoptosis assay of parental, K562-Cas9 and -K562-*ABL*-TK cells. (B) Quantification of annexin-V labeling in cell populations (mean ± SEM; *** $p<0.001$). (C) DNA content analysis of cell populations.

Figure 5.- CRISPR/Cas9 deletion system in mouse leukemic stem cells. Mouse leukemic stem cells (mLSCs) were isolated from TgP210+ mouse bone marrow, and electroporated with Cas9 and with Cas9 joined to both sgRNAs (*ABL*-TK). (A) PCR-amplification of the genomic ABL exon 6 sequence and Sanger sequencing. (B) Quantitative PCR of *BCR/ABL* mRNA (fusion point) and *ABL* mRNA (exon 7-8) in mLSC-Cas9 (control) and mLSC-*ABL*-TK (edited) cells (mean ± SEM; ***$p<0.001$). (C) Anti-human ABL immunostaining of mLSC mouse cells.

Figure 6.- Engraftment and Multipotency capacity of CRISPR/Cas9 edited mLSCs. (A) Schematic representation of the experimental procedure and study groups.

(B) 4 months after BMT, mouse $CD45^+$ cell populations from peripheral blood were analyzed and isolated by FACS. Lymphoid ($B220^+$, $CD4^+$, and $CD8^+$) and myeloid ($Gr1^+$ and $Mac1^+$) populations were identified in the blood samples. (C) DNA samples from $mCD45^+$ cells from mLSC-Cas9 and mLSC-*ABL*-TK mice were PCR-amplified, revealing the presence of a CRIPSPR/Cas9-induced deletion in *ABL* exon 6 of the $GR1^+$, $B220^+$, $CD4^+$, $CD8^+$ and SCA^+ cells. (D) Quantification of *BCR/ABL* expression in recovered mCD45 cells 4 months after transplantation (mean ± SEM; ***p<0.001).

Figure 7.- Therapeutic evaluation of CRISPR/Cas9 deletion system in a Mouse model of LMC. (A) Schematic representation of the experimental procedure and study groups. (B) Macroscopic aspect and spleen sizes of CML transgenic mice, wild-type mice, and NSG recipient mice (NSG-Cas9 and NSG-*ABL*-TK). (C) FACS quantification of Gr1-positive cells and representative micrography of hematoxylin-stained peripheral blood. **(D)** FACS analysis of myeloid and lymphoid hematological populations generated in peripheral blood of NSG recipient mice after BMT: NSG-*ABL*-TK; (pink box), NSG-Cas9 (red box). CML transgenic mice (black box) and wild-type mice (grey box) were used as controls for CML disease and normal cell distribution (median ± SEM; *p<0.05; **p<0.01; ***p<0.001). **(E)** Percentage and evolution of $Gr1^+$ cell population analyzed in peripheral blood of NSG recipients with mLSC engraftments from CML transgenic mice at different stages disease. mLSCs were divided into two groups with the same number and were electroporated with Cas9 (NSG-Cas9, red line) and with Cas9 joined to both sgRNAs (NSG-*ABL*-TK, blue line) before BMT.

Figure 8.- Effects of CRISPR/Cas9 deletion system in human LSCs.
Human $CD34^+$ LSCs were isolated from bone marrow biopsies of CML patients, and electroporated with/without the all CRISPR/Cas9 reagents. **(A)** PCR amplification of ABL exon 6 in hLSC from patients electroporated with Cas9 nuclease (hLSC-Cas9) and Cas9 joined to both sgRNAs (hLSC-*ABL*-TK). Sanger sequencing of ABL exon 6 of both cell populations. **(B)** Quantitative PCR of *BCR/ABL* (fusion *BCR/ABL* exons, left) and *ABL* (exon 7-8, right) (mean ± SEM; *** p<0.001). **(C)** Western blot anti-ABL in hLSC cells. Cells electroporated with Cas9, used as control, showed a single band corresponding to ABL (~135 kDa). However, hLSC electroporated with *ABL*-TKs showed a lower level expression level of ABL protein. **(D)** *In vitro* cell proliferation and apoptosis analysis of hLSC after CRISPR/Cas9 editing. LSC proliferation and apoptosis levels were measured 24, 48 and 96 h after electroporation with Cas9 (red) and Cas9 joined to ABL-TK sgRNAs (blue). hLSC-*ABL*-TK showed a lower proliferation ability and a higher apoptosis rate than non-edited cells (hLSC-Cas9).

Figure 9.- Multipotency capacity and therapeutic evaluation of CRISPR-edited hLSCs in an orthotopic model. Human $CD34^+$ LSCs were isolated from bone marrow biopsies of CML patients, electroporated with/without all CRISPR/Cas9 reagents and transplanted into irradiated NSG mice. **(A)** Schematic representation of study groups and experimental procedure. **(B)** FACS analysis of human hematological cell

populations in bone marrow 24 weeks after BMT. NSG with hLSC engraftments from patients electroporated with Cas9 nuclease are named NSG-hLSC-Cas9. NSG with hLSC engraftments from patients electroporated with Cas9 joined both sgRNAs are named NSG-hLSC-*ABL*-TK. **(C)** Quantitative PCR of *BCR/ABL* (fusion *BCR/ABL* exons, left) and *ABL* (exon 7-8, right) in hCD45 cells from NSG bone marrow 24 weeks after BMT. **(D)** FACS analysis of human hematological $hCD45^{+}$ cell population 24 weeks after BMT in NSG mice. NSG with hLSCs engraftments electroporated with Cas 9 are named NSG-hLSC-*Cas9* (red boxes) and with Cas9 joined to sgRNAs are named hLSC-*ABL*-TK (pink boxes). NSG with healthy $hCD34^{+}$ engraftments (NSG-healthy-$hCD34^{+}$, grey boxes) were used as normal controls. NSG with untreated $hCD34^{+}$ cells from CML patient (NSG-hLSC-$CD34^{+}$; black boxes) were used as a control disease. (***$p<0.001$). **(E)** Linear regression analysis of hCD117+ and hCD19+ cell populations in the NSG mice engraftments. NSG with hLSCs engraftments electroporated with Cas 9 are represented with pink dots, with Cas9 joined to sgRNAs are represented with red dots. NSG with healthy $hCD34^{+}$ engraftments (NSG-healthy-$hCD34^{+)}$ are represented with grey boxes. NSG with untreated $hCD34^{+}$ cells from CML patient (NSG-hLSC-$CD34^{+}$) are represented with black boxes.

Figure S1.- Experimental design of the CRISPR/Cas9 system for blocking the *BCR/ABL* fusion oncogene. Detail of fusion *BCR/ABL* gene resulting from t(9:22) and the expected cleavage point of sgRNA against *ABL* exon 6. The resulting 101-bp deletion would generate a premature stop codon in exon 7.

Table S1.- Oligonucleotides

	Sequence
ABLTK-F	TCCATTATCCAGCCCCAAAGCG
ABLTK-R	GATGGGGAACTTGGCTCCAGC
ABL ex6 F	AGTCAGAATCCTTCAGAAGGCT
ABL ex6 R	CTGAATTTAGCCCTGGATGCAT
***BCR/ABL* qPCR F**	TTTCTGAATGTCATCGTCC
***BCR/ABL* qPCR R**	TTGGGCTTCACACCATTCCCC
ABL ex7 qPCR F	GTCCGACGTCTGGGCATTTG
ABL ex8 qPCR R	GCTCGCATGAGTTCATAGACC
***Gapdh* qPCR F**	TGCACCACCAACTGCTTAGC
***Gapdh* qPCR R**	CACCACCTTCTTGATGTCATCA

Table S2.- mLSC Donor mice used for mice-mice bone marrow transplantations.

	ID	NSG	%Gr1$^+$	%B220$^+$	Age (months)	Gender
CML-Tg mice	9974		77.1	10.6	12	M
(n=5)	10309		48.8	8	10	F
	10819		51.8	27.4	9	M
	10979		62.6	6.6	11	M
	10978		85.7	3.17	11	M
WT mice	18016		17.4	37.6	9	F
(n=5)	10315		16	33.8	6	M
	10316		12.6	33.8	10	F
	9632		12.7	63.8	6	M
	9444		30.8	63.4	6	M
mLSC donors	7802	1/2	65.2	11.5	16	F
(n=6)	9451	3/4	81.5	3.1	14	F
	9977	5/6	63.7	1.9	13	M
	9976	7/8	63.9	5.9	13	M
	9450	9/10	64.8	6.6	14	F
	9783	11/12	77.3	10.6	12	F
mLSC donors	9784	Donor#1	35.4	38.5	12	F
(n=3)	10981	Donor#2	52.3	12.4	10	F
	10817	Donor#3	68.8	3.2	11	M

Table S4.- FACS Analysis of peripheral blood of NSG mice 16 weeks after mLSC transplantation.

	ID	%Mac1$^+$	%Gr1$^+$	%Mac1$^+$Gr1$^+$	%B220$^+$	IgM$^+$	CD4$^+$	CD8$^+$
CML-Tg mice	9974	51.0	77.1	61.6	10.6	5.8	2.5	2.2
n=5	10309	65.9	48.8	42.3	8	29.7	6.3	9.5
	10819	50.7	51.8	45.8	27.4	25.1	8.9	8.4
	10979	53.0	62.6	48.2	6.6	2.9	4.9	1.8
	10978	77.0	85.7	72.8	3.17	0.7	2.8	0.9
NSG-Cas9	1	59.5	49.7	33.1	9.9	13.9	18.8	8.7
n=6	3	24.8	31.6	20.1	1.0	20.0	34.5	19.4
	5	64.1	73.0	44.9	2.5	1.5	0.9	0.9
	7	54.5	89.3	49.4	6.3	10.5	2.9	4.5
	9	72.9	52.3	44.0	2.0	1.5	7.9	9.1
	11	63.2	67.5	40.2	4.0	1.8	2.8	1.8
WT mice	18016	21.8	17.4	15.9	37.6	30.7	17.8	16.3
n=5	10315	21.6	16	12.8	33.8	27.6	23.2	19.9
	10316	16.8	12.6	10.4	33.8	26.2	26.2	19.2
	9632	15.1	12.7	10.2	63.8	42.7	21.3	13.9
	9444	22.7	30.8	19.9	63.4	21.7	25.8	13.0
NSG-ABL-TK	2	43.7	52.1	32.1	13.9	10.1	12.3	6.3
n=6	4	11.9	17.9	7.2	1.0	28.8	40.9	21.2
	6	38.0	35.2	22.6	27.9	13.0	11.7	5.8
	8	38.0	17.1	15.0	27.9	6.9	33.2	16.2
	10	26.9	24.0	19.0	39.5	23.6	17.9	13.9
	12	29.0	26.6	14.5	33.5	12.0	19.2	15.5

Table S5.- FACS Analysis of bone marrow hematological populations in NSG mice 24 weeks after hLSC transplantation.

	ID	%CD34$^+$	%CD14$^+$	%CD117$^+$	%CD19$^+$
NSG-hLSC CD34	13	27.0	4.6	92.7	26.5
n=3	14	12.8	3.8	62.0	22.6
	15	11.3	50.0	85.1	12.3
NSG- hLSC-Cas9	16	0.5	14.4	91.0	5.2
n=7	17	2.9	20.6	91.9	6.6
	18	23.9	34.2	85.9	20.5
	19	9.9	94.7	97.0	7.3
	20	29.6	89.5	62.0	30.4
	21	18.6	64.4	90.9	12.2
	22	18.1	87.3	91.1	13.5
NSG-healthy CD34	23	11.3	0.7	0.9	92.3
n=3	24	1.8	0.9	1.6	94.9
	25	3.2	1.8	2.1	91.1
NSG-hLSC-*ABL*-TK	26	35.6	7.8	4.3	70.5
n=7	27	1.9	16.3	9.2	84.0
	28	4.4	1.6	0.2	95.8
	29	0.5	7.2	23.7	82.4
	30	0.1	0.1	0.3	95.9
	31	0.1	0	55.4	80.9
	32	9.7	4.3	1.7	84.7